Project Number 260041

SUPPORTING ACTION

EnRiMa

Energy Efficiency and Risk Management in Public Buildings

Deliverable D2.2: A Mathematical Formulation of Energy Balance and Flow Constraints

Start date of the project: 01/10/2010

Duration: 42 months

Organisation name of lead contractor for this deliverable: UCL

Revision: 30 March 2012

Project funded by the European Commission within the Seventh Framework Programme (2007-2013)		
Dissemination Level		
PU	Public	**X**
PP	Restricted to other programme participants (including the Commission Services)	
RE	Restricted to a group specified by the consortium (including the Commission Services)	
CO	Confidential, only for members of the consortium (including the Commission Services)	

Contents

List of Figures

List of Tables

List of Acronyms

AHU Air-handling unit

BHHW Building heating and hot water

BMS Building management system

CAC Cooling and conditioning

CHP Combined heat and power

CS Circulation system

DER Distributed energy resources

DER-CAM DER Customer Adoption Model

DG Distributed generation

DHW Domestic hot water

DIN Deutsches Institut für Normung

DoW Description of Work

DSS Decision Support System

DV Decision variable

EnRiMa Energy Efficiency and Risk Management in Public Buildings

EU European Union

FASAD Fundación Asturiana de Atención y Protección a Personas con Discapacidades y/o Dependencias

FTP File Transfer Protocol

HWH Hot water for heating

HVAC Heating, ventilation, and air conditioning

ICT Information and communication technologies

IL Indoor illumination

MCEEM Microgrid Customer Engineering-Economic Model

MT Microturbine

NG Natural gas

NGB Natural gas boiler

OTH Other uses

PV Photovoltaic

RE Reciprocating engine

RTE Regulated tariff for electricity

RTG Regulated tariff for natural gas

RTH Regulated tariff for district heating

SMS Symbolic model specification

SRC Server room conditioning

TOU Time of use

TRV Thermostatic radiator control valve

WP Work Package

Executive Summary

Improving energy efficiency in public buildings requires an accurate representation of how energy produced by resources flows to loads. This link between loads and resources not only aids visualisation of energy flows in buildings but also serves as constraints in mathematical programs that optimise operational and strategic decisions. The former concern the dispatch levels of existing technologies in meeting fixed loads and/or the comfort levels of users on a short-term, e.g., hourly, basis. Meanwhile, the latter focus on adoption of new technologies, replacement of existing technologies, and retrofits to the building. Since the viability of such investment and capital-improvement decisions depends on the use of technologies over the long term, energy balances have to be expressed at an aggregate level. Building on the Sankey diagrams and initial energy-balance relations developed in Deliverable D2.1, we devise energy-balance constraints that will be used for both operational and strategic decision making as part of the symbolic model specification in Deliverable D4.2. In particular, our extension to the existing state-of-the-art at the operational level is to loosen the traditional definition of demand for heating or cooling and to consider instead user requirements for temperature. This leads to lower-level energy-balance constraints that reflect the thermodynamics of heating and cooling systems as well as building physics. By implementing these constraints as part of an operational optimisation for the two test sites, we illustrate how they work and demonstrate our approach's potential for reducing energy consumption. Our preliminary results indicate that optimising the operations of conventional heating and HVAC systems may reduce energy consumption by up to 10%. At the strategic level, we maintain fixed loads for all energy end uses, but we adapt our constraints to consider retrofits and passive measures. Using the energy-transfer efficiencies between each load-resource pair, we show how energy-transfer matrices may be automated to produce updated information in the form of Sankey diagrams. In order to demonstrate the advantages of our approach, we illustrate the lower-level energy-balance constraints with optimisation examples based on current configurations at each test site and show the automation of energy-transfer efficiencies via a Web-based tool.

1 Introduction

In order to improve energy efficiency and provide adequate risk management to users of public buildings in the European Union (EU), the EnRiMa project takes a flexible solution approach based on energy-flow modelling and stochastic optimisation integrated with information and communication technologies (ICT). The advantage of an optimisation perspective is that it enables the adoption and operation of a diverse set of resources to meet a variety of end-use energy demands. By adapting well-known methods for large-scale optimisation (Hobbs, 1995), we exploit their logic while adjusting for building-level details such as combined heat and power (CHP), storage technologies, passive measures, and operational thermodynamics at the lower level. Crucial to this effort is modelling the energy flows at each test site, which began with construction of the Sankey diagrams in Deliverable D2.1 (UCL et al., 2011). In that document, we calculated energy-transfer efficiencies that facilitated our objective of mapping energy flows. In tandem, we also developed rudimentary energy-balance constraints for existing configurations at the two test sites and one back-up site.

Using the platform established by Deliverable D2.1 along with the information about the test sites' configurations and system requirements from Deliverables D1.1 and D4.1 (HCE et al. (2011) and IIASA et al. (2011)), we develop formal energy-balance constraints in this document, which will be used as part of the symbolic model specification (SMS) in the concurrent Deliverable D4.2. Taking the approach of Hobbs (1995), we generalise the energy-balance constraints from the literature on distributed generation, viz., King and Morgan (2007) and Marnay et al. (2008). In particular, we develop energy-balance constraints at both the upper and lower levels given existing financial positions and system configurations. The distinction between the two is that the former takes end-use energy demands as fixed with no explicit representation of building physics or the thermodynamics of conventional heating or HVAC systems. Instead, the upper-level constraints are meant to reflect energy balances at a level of detail that would be suitable for capturing operational effects as part of a strategic optimisation module, i.e., one in which strategic decision variables such as equipment installations, financial positions, and retrofits involving passive measures are the focus. Upper-level operational decisions, e.g., dispatch of installed equipment and energy purchases or sales in short-term markets, would also be included in the strategic module. By contrast, lower-level constraints do not have explicit end-use demands for space heat and cooling; rather, they assume that the building operator sets desired zone temperatures (or ranges) for each short-term decision-making period. Next, given the external temperature, characteristics of the building envelope, solar gains, internal loads, and the thermodynamics of the conventional heating and HVAC systems, lower-level operational decisions regarding the dispatch of radiators or ventilation change the zone temperature to keep it at the desired target level or range. Thus, end-use energy demands for certain types of heating and cooling are variables because they are determined endogenously. These lower-level energy-balance constraints together with the lower-level decision variables may be run independently or in conjunction with the upper-level energy-balance constraints and operational decision variables to constitute the operational module. The philosophy of the EnRiMa DSS is indicated in Fig. 1. A strategic module focuses on equipment investment, financial hedging, and site retrofit decisions taking operational decisions and energy flows into account at a high level. By this, we mean that building physics and heating/cooling system thermodynamics are not modelled, and end-use energy demands are exogenous. However, passive measures for reduc-

ing end-use energy consumption in the future are available as portfolios whose effectiveness is based on a building model and calculated offline. At the lower level, an operational module models building physics and system thermodynamics in order to make certain end-use energy demands (such as those for space heat and cooling) endogenous. On the other hand, the operational module takes installed equipment, the building envelope, and financial positions as given.

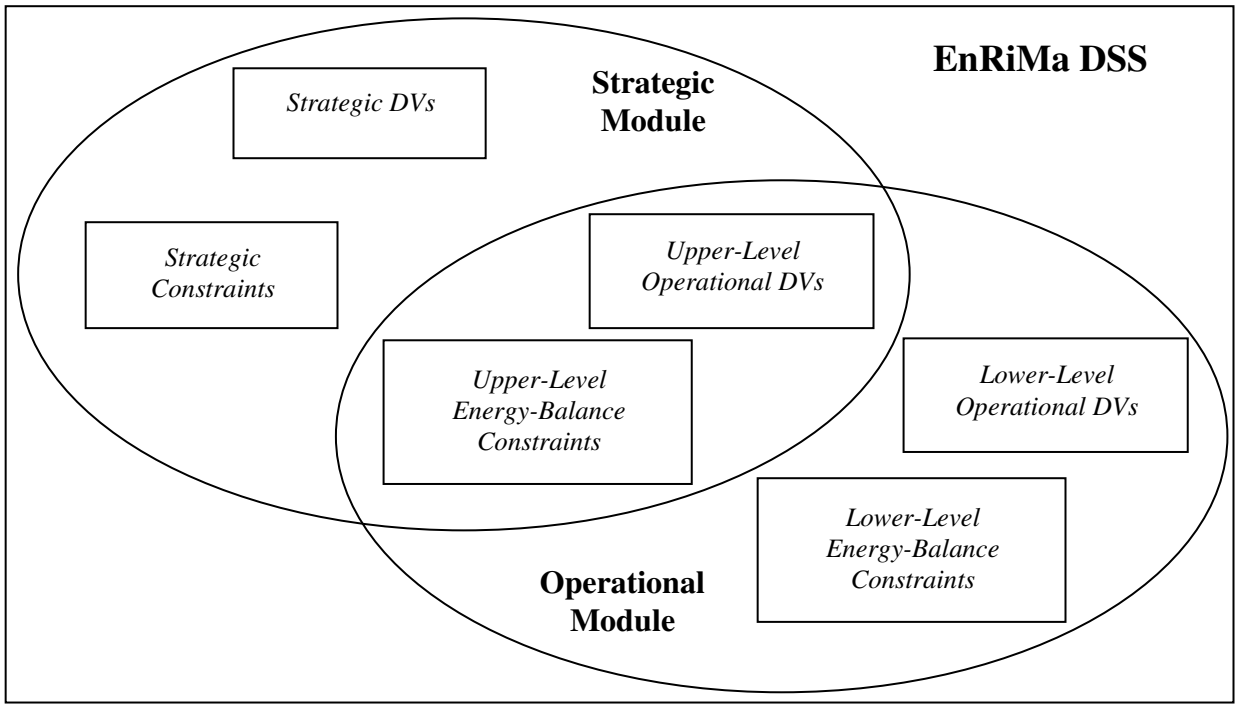

Figure 1: EnRiMa DSS Schema

The work outlined in this deliverable contributes to Operational Objective O1 of the EnRiMa DoW by considering the impact of equipment upgrades and passive measures on energy-efficiency improvement and cost reduction. These features are modelled in Section 2 with details on passive measures available in Appendix B. The other aspect of Operational Objective O1 is met by treating explicitly the effect of building characteristics, prices, user preferences for comfort, and weather on end-use energy demand. These lower-level features are modelled in Section 3. In both cases, we endeavour to implement the energy-balance constraints at our two test sites either to demonstrate that their logic is consistent with observed energy flows (at the upper level) or to illustrate their potential in reducing energy consumption as part of an optimisation (at the lower level). Another enhancement to the existing state-of-the-art for modelling energy flows that is accomplished in this deliverable is an automated procedure for calculating energy-transfer efficiency matrices (see Appendix A), which are used to implement the upper-level energy-balance constraints and create Sankey diagrams for various time periods. Finally, we assume that all installed equipment operates at constant efficiencies for large ranges of the output, a feature that we observe empirically for small-scale technologies and document in Appendix C.

The structure of this document is as follows:

- Section 2 constructs upper-level energy-balance constraints in a flexible way to ensure

adaptability to most building types and demonstrates their logic by implementing them for the two EnRiMa test sites.

- Section 3 takes an expansive view of end-use energy demand for space heat and cooling by devising lower-level energy-balance constraints that reflect building physics and system thermodynamics. These constraints are implemented as part of an operational optimisation for the two test sites in order to illustrate how they work and to demonstrate our approach's potential for reducing energy consumption. Our preliminary results indicate that optimising the operations of conventional heating and HVAC systems may reduce energy consumption by up to 10% relative to the current level.
- Section 4 summarises the work of this document, discusses its limitations, and explains how it links with the work in other concurrent and forthcoming deliverables.
- Appendix A documents the procedure for calculating energy-transfer efficiencies in a structured way in order to create Sankey diagrams.
- Appendix B explains how the effectiveness of passive measures is estimated for use in the upper-level constraints of Section 2.
- Appendix C provides empirical evidence for why we feel that it is justified to assume constant energy-conversion efficiencies for on-site technologies. Nevertheless, we provide a stylised formulation that reflects how energy efficiency of an on-site generator may vary with the operating level.

2 Upper-Level Energy Balance

2.1 Overview

At the upper level, we abstract from details about building physics (except to capture the effects of passive measures for demand reduction) and heating/cooling system thermodynamics. Thus, we take end-use energy demands as fixed along with the current site configuration, i.e., the installed equipment, financial positions, and the building envelope, in order to derive the upper-level energy-balance constraints. These may be embedded with the strategic constraints in order to formulate the mathematical program that serves as the basis for the strategic module of the EnRiMa DSS, which is the focus of the concurrent Deliverable D4.2.

The schema in Fig. 2 indicates the possible flow of energy to/from external/internal sources and sinks. We denote three types of sets in the schema: energy markets (grey), energy types (blue), and energy technologies (pink). Energy markets are sources for procuring various types of energy. For example, we may have electricity markets and district heating for processed energy types such as electricity and hot water, and markets for various primary fuels, such as biomass or natural gas, which may be used to run on-site equipment. Energy may also be sold back to some markets, e.g., electricity. In addition, we have fictitious markets: the sun (for free solar energy) and venting (for free release of hot air produced on site).

Energy procured from each market may be used either directly to meet end-use demand at the site or indirectly as input to create another type of energy via one of the energy-creating technologies. For example, fuel may be used in the boiler (producing hot water), the on-site generation unit (producing electricity and hot water), and the direct-fired chiller

(producing cooling). Subsequently, the hot water may be used for consumption or as input to the heat exchanger (absorption chiller) to produce space heat (cooling), while the electricity may be consumed directly, sold into markets, or used to run other on-site equipment, e.g., heat pumps. Furthermore, energy-storage technologies, such as batteries or hot water tanks, enable the desynchronisation of energy's production from its subsequent consumption albeit with storage losses. Given time-varying energy prices, energy-storage technologies may provide an attractive pathway to improve a site's economic, efficiency, and emissions metrics. Since passive technologies are not dispatchable and simply reduce the quantity demanded of each type of eligible end-use energy demand, they are not explicitly shown in Fig. 2.

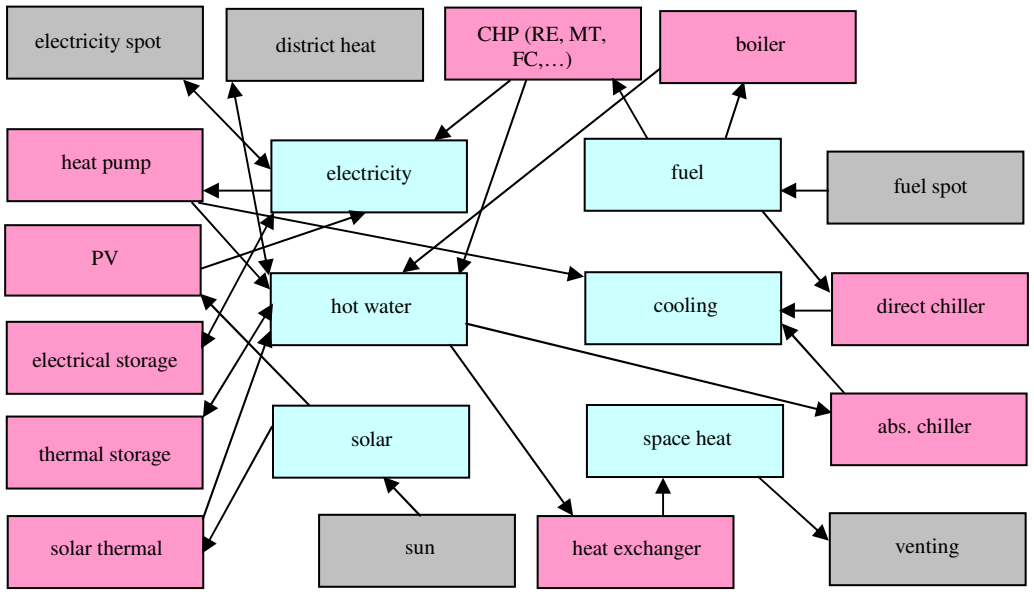

Figure 2: Schema of Strategic-Level Energy Flows

2.2 Nomenclature

Next, we describe the nomenclature used throughout this deliverable, viz., indices, sets, parameters, and variables.

2.2.1 Indices

- $n \in \mathcal{N}$: energy market
- $p \in \mathcal{P}$: long-term period
- $m \in \mathcal{M}$: mid-term period (also $mm \in \mathcal{M}$)
- $t \in \mathcal{T}$: short-term period
- $i \in \mathcal{I}$: energy-creating technology
- $j \in \mathcal{J}$: energy-absorbing technology or passive-measure portfolio
- $k \in \mathcal{K}$: energy type (also $kk \in \mathcal{K}$)

- $\ell \in \mathcal{L}$: pollutant

2.2.2 Sets

- $\mathcal{N} \supset \mathcal{N}_E \cup \mathcal{N}_H \cup \mathcal{N}_G \cup \mathcal{N}_D$: markets for energy products and primary fuels
  - $\mathcal{N}_{B,k} \subset \mathcal{N}$: markets from which energy type $k \in \mathcal{K}$ may be bought
    - $\mathcal{N}_{B,P,k} \subset \mathcal{N}_{B,k}$: markets from which processed energy type $k \in \mathcal{K}$ may be bought
    - $\mathcal{N}_{B,F,k} \subset \mathcal{N}_{B,k}$: forward markets from which energy type $k \in \mathcal{K}$ may be bought
  - $\mathcal{N}_{S,k} \subset \mathcal{N}$: markets into which energy type $k \in \mathcal{K}$ may be sold
    - $\mathcal{N}_{S,F,k} \subset \mathcal{N}$: forward markets into which energy type $k \in \mathcal{K}$ may be sold
  - $\mathcal{N}_E \supset \mathcal{N}_{E,U} \cup \mathcal{N}_{E,S} \cup \mathcal{N}_{E,F}$: electricity markets
    - $\mathcal{N}_{E,U}$: utility at tariff rate
    - $\mathcal{N}_{E,S}$: spot markets
    - $\mathcal{N}_{E,F}$: forward markets
  - $\mathcal{N}_D$: fictitious markets
  - $\mathcal{N}_H$: heating markets
  - $\mathcal{N}_G \supset \mathcal{N}_{G,U} \cup \mathcal{N}_{G,S} \cup \mathcal{N}_{G,F}$: natural gas markets
    - $\mathcal{N}_{G,U}$: utility at tariff rate
    - $\mathcal{N}_{G,S}$: spot markets
    - $\mathcal{N}_{G,F}$: forward markets
- $\mathcal{I} \supset \mathcal{I}_E \cup \mathcal{I}_H \cup \mathcal{I}_C$: energy-creating technologies
  - $\mathcal{I}_E = \mathcal{I}_{E,C} \cup \mathcal{I}_{E,D}$: electricity-generating technologies
    - $\mathcal{I}_{E,C}$: electricity-generating technologies available in continuous sizes
    - $\mathcal{I}_{E,D}$: electricity-generating technologies available in discrete sizes
  - $\mathcal{I}_H = \mathcal{I}_{H,C} \cup \mathcal{I}_{H,D}$: heat-producing technologies
    - $\mathcal{I}_{H,C}$: heat-producing technologies available in continuous sizes
    - $\mathcal{I}_{H,D}$: heat-producing technologies available in discrete sizes
  - $\mathcal{I}_C$: cooling technologies
- $\mathcal{J} \supset \mathcal{J}_P \cup \mathcal{J}_S$: energy-absorbing technologies
  - $\mathcal{J}_P$: passive-measure portfolios
  - $\mathcal{J}_S$: storage technologies
- $\mathcal{K} \supset \mathcal{K}_E \cup \mathcal{K}_H \cup \mathcal{K}_C \cup \mathcal{K}_G \cup \mathcal{K}_S$: energy types
  - $\mathcal{K}_{I,i} \subset \mathcal{K}$: input energy types for energy-creating technology $i \in \mathcal{I}$
  - $\mathcal{K}_{O,i} \subset \mathcal{K}$: output energy types for energy-creating technology $i \in \mathcal{I}$
  - $\mathcal{K}_E$: electricity
  - $\mathcal{K}_H$: heat

  - $\mathcal{K}_C$: cooling
  - $\mathcal{K}_G$: natural gas
  - $\mathcal{K}_S$: solar
- $\mathcal{P}$: long-term periods for strategic decisions
- $\mathcal{M}$: mid-term representative periods
  - $\mathcal{A}_{k,n}^{p,m,t}$: ancestor mid-term periods for purchase of energy type $k \in \mathcal{K}$ from market $n \in \mathcal{N}_{B,k}$ for delivery during $p \in \mathcal{P}$, $m \in \mathcal{M}$, $t \in \mathcal{T}$ (note that $\mathcal{A}_{k,n}^{p,m,t} = m$ for $n \notin \mathcal{N}_{B,F,k}$)
  - $\mathcal{S}_{k,n}^{p,m,t}$: ancestor mid-term periods for sale of energy type $k \in \mathcal{K}$ to market $n \in \mathcal{N}_{S,k}$ for delivery during $p \in \mathcal{P}$, $m \in \mathcal{M}$, $t \in \mathcal{T}$ (note that $\mathcal{S}_{k,n}^{p,m,t} = m$ for $n \notin \mathcal{N}_{S,F,k}$)
- $\mathcal{T}$: short-term periods for operational decisions
- $\mathcal{L}$: pollutants

2.2.3 Parameters

- HO: number of operating periods
- EF: required energy efficiency of the site (unitless)
- $B_{k,n}$: units of primary energy required to make one unit of energy type $k \in \mathcal{K}$ available from market $n \in \mathcal{N}_{B,k}$ (kWh/kWh or kWh/kWh$_e$)
- $C_{k,\ell,n}$: mean rate of emission of pollutant $\ell \in \mathcal{L}$ from processed energy type $k \in \mathcal{K}$ purchased from market $n \in \mathcal{N}_{B,P,k}$ (kg/kWh or kg/kWh$_e$)
- $H_{i,k,\ell}$: rate of emission of pollutant $\ell \in \mathcal{L}$ from energy-creating technology $i \in \mathcal{I}$ using energy input $k \in \mathcal{K}_{I,i}$ (kg/kWh or kg/kWh$_e$)
- DT: length of decision-making period (hours)
- $0 \leq A_i^{p,m,t} \leq 1$: availability of energy-creating technology $i \in \mathcal{I}$ during period $p \in \mathcal{P}$, $m \in \mathcal{M}$, $t \in \mathcal{T}$ (this is binary for all technologies besides PV)
- CI_i: lump-sum capital cost of electricity-generating technology $i \in \mathcal{I}_E$ (€/kW$_e$), heat-producing technology $i \in \mathcal{I}_H$ (€/kW), or cooling technology $i \in \mathcal{I}_C$ (€/kW)
- CO_i: non-fuel operating and maintenance cost of electricity-generating technology $i \in \mathcal{I}_E$ (€/kWh$_e$), heat-producing technology $i \in \mathcal{I}_H$ (€/kWh), or cooling technology $i \in \mathcal{I}_C$ (€/kWh)
- $D_k^{p,m,t}$: end-use energy demand for $k \in \mathcal{K}_E$ (kWh$_e$), $k \in \mathcal{K}_C$ (kWh), or $k \in \mathcal{K}_H$ (kWh) during period $p \in \mathcal{P}$, $m \in \mathcal{M}$, $t \in \mathcal{T}$
- $E_{i,k,kk}$: units of energy type $k \in \mathcal{K}_{I,i}$ needed to produce one unit of energy type $kk \in \mathcal{K}_{O,i}$ via electricity-generating technology $i \in \mathcal{I}_E$ (kWh/kWh$_e$), heat-producing technology $i \in \mathcal{I}_H$ (kWh/kWh), or cooling technology $i \in \mathcal{I}_C$ (kWh/kWh)
- $F_i \in \mathcal{K}_{O,i}$: principal energy output of energy-creating technology $i \in \mathcal{I}$

- $0 \leq OA_{k,j} \leq OB_{k,j} \leq 1$: lower and upper limits on the fraction of capacity of energy-storage technology $j \in \mathcal{J}_S$ that must be charged with energy type $k \in \mathcal{K}$
- $0 \leq OD_{k,j} \leq 1$: proportion of end-use demand of energy type $k \in \mathcal{K}$ reduced for each unit of passive-measure portfolio $j \in \mathcal{J}_P$ available (based on the site's current configuration, see Appendix B for details on how this parameter is calculated)
- $0 \leq OI_{k,j} \leq 1$: units of energy type $k \in \mathcal{K}$ available for each unit sent to energy-storage technology $j \in \mathcal{J}_S$ (kWh/kWh or kWh_e/kWh_e)
- $OO_{k,j} \geq 1$: units of energy type $k \in \mathcal{K}$ needed to be discharged from energy-storage technology $j \in \mathcal{J}_S$ in order to produce one unit of usable energy (kWh/kWh or kWh_e/kWh_e)
- $0 \leq OR_{k,j} \leq 1$: units of energy type $k \in \mathcal{K}$ available for discharge for each unit stored in energy-storage technology $j \in \mathcal{J}_S$ (kWh/kWh or kWh_e/kWh_e)
- $0 \leq OS_{k,j} \leq 1$: units of energy type $k \in \mathcal{K}$ available for each unit stored after each short-term time period in energy-storage technology $j \in \mathcal{J}_S$ (kWh/kWh or kWh_e/kWh_e)
- G_i: capacity of discrete-sized electricity-generating technology $i \in \mathcal{I}_{E,D}$ (kW_e)

2.2.4 Decision Variables

- $e^{p,m,t}$: energy consumption of site during period $p \in \mathcal{P}$, $m \in \mathcal{M}$, $t \in \mathcal{T}$ (kWh)
- $qo_{k,j}^{p,m,t}$: release from energy-storage technology $j \in \mathcal{J}_S$ of energy type $k \in \mathcal{K}$ during period $p \in \mathcal{P}$, $m \in \mathcal{M}$, $t \in \mathcal{T}$ (kWh_e or kWh)
- $qi_{k,j}^{p,m,t}$: addition to energy-storage technology $j \in \mathcal{J}_S$ of energy type $k \in \mathcal{K}$ during period $p \in \mathcal{P}$, $m \in \mathcal{M}$, $t \in \mathcal{T}$ (kWh_e or kWh)
- $r_{k,j}^{p,m,t}$: storage of energy type $k \in \mathcal{K}$ in energy-storage technology $j \in \mathcal{J}_S$ during period $p \in \mathcal{P}$, $m \in \mathcal{M}$, $t \in \mathcal{T}$ (kWh_e or kWh)
- $u_{k,n}^{p,m,t,mm}$: purchase of energy type $k \in \mathcal{K}$ from market $n \in \mathcal{N}_{B,k}$ during mid-term period $mm \in \mathcal{A}_{k,n}^{p,m,t}$ for delivery in $p \in \mathcal{P}$, $m \in \mathcal{M}$, $t \in \mathcal{T}$ (kWh_e or kWh)
- $v_\ell^{p,m,t}$: output of pollutant $\ell \in \mathcal{L}$ during period $p \in \mathcal{P}$, $m \in \mathcal{M}$, $t \in \mathcal{T}$ (kg)
- $w_{k,n}^{p,m,t,mm}$: sale of energy type $k \in \mathcal{K}$ to market $n \in \mathcal{N}_{S,k}$ during mid-term period $mm \in \mathcal{S}_{k,n}^{p,m,t}$ for delivery in $p \in \mathcal{P}$, $m \in \mathcal{M}$, $t \in \mathcal{T}$ (kWh_e or kWh)
- s_i^p: number of units of discrete-sized electricity-generating technology $i \in \mathcal{I}_{E,D}$ available at time $p \in \mathcal{P}$
- s_i^p: capacity of energy-creating technology $i \in \mathcal{I}_{E,C} \cup \mathcal{I}_H \cup \mathcal{I}_C$ available at time $p \in \mathcal{P}$ (kW_e or kW)
- x_j^p: storage capacity of energy-storage technology $j \in \mathcal{J}_S$ available at time $p \in \mathcal{P}$ (kWh_e or kWh) or indicator for installation of passive-measure portfolio $j \in \mathcal{J}_P$ available at time $p \in \mathcal{P}$ (binary)
- $y_{i,k}^{p,m,t}$: input of energy type $k \in \mathcal{K}$ to energy-creating technology $i \in \mathcal{I}$ during period $p \in \mathcal{P}$, $m \in \mathcal{M}$, $t \in \mathcal{T}$ (kWh_e or kWh)

- $z_{i,k}^{p,m,t}$: output of energy type $k \in \mathcal{K}$ from energy-creating technology $i \in \mathcal{I}$ during period $p \in \mathcal{P}$, $m \in \mathcal{M}$, $t \in \mathcal{T}$ (kWh_e or kWh)

2.3 Constraints

The energy-balance constraints are described in this section.

$$\sum_{i \in \mathcal{I}} y_{i,k}^{p,m,t} + \sum_{mm \in \mathcal{S}_{k,n}^{p,m,t}} \sum_{n \in \mathcal{N}_{S,k}} w_{k,n}^{p,m,t,mm} + D_k^{p,m,t} \cdot \left(1 - \sum_{j \in \mathcal{J}_P} OD_{k,j} \cdot x_j^p\right) + \sum_{j \in \mathcal{J}_S} qi_{k,j}^{p,m,t}$$
$$= \sum_{i \in \mathcal{I}} z_{i,k}^{p,m,t} + \sum_{mm \in \mathcal{A}_{k,n}^{p,m,t}} \sum_{n \in \mathcal{N}_{B,k}} u_{k,n}^{p,m,t,mm} + \sum_{j \in \mathcal{J}_S} qo_{k,j}^{p,m,t}, \forall\ k \in \mathcal{K}, p \in \mathcal{P}, m \in \mathcal{M}, t \in \mathcal{T} \quad (1)$$

Eq. 1 states that during each time period the use of each energy type, whether as input to energy-creating technologies, sales to markets, consumption after the effect of any passive measures, or charging of storage, must equal its availability, whether from on-site production, purchase from markets, or discharging from storage.

$$z_{i,F_i}^{p,m,t} \leq DT \cdot A_i^{p,m,t} \cdot G_i \cdot s_i^p,$$
$$i \in \mathcal{I}_{E,D} \cup \mathcal{I}_{H,D} \cup \mathcal{I}_{C,D}, \forall\ p \in \mathcal{P}, m \in \mathcal{M}, t \in \mathcal{T} \quad (2)$$

Eq. 2 constrains the amount of each principal energy type, i.e., that for which F_i is the principal energy output of technology i, that is available during each time period from each discrete-sized technology by its installed capacity.

$$z_{i,F_i}^{p,m,t} \leq DT \cdot A_i^{p,m,t} \cdot s_i^p,$$
$$i \in \mathcal{I}_{E,C} \cup \mathcal{I}_{H,C} \cup \mathcal{I}_{C,C}, \forall\ p \in \mathcal{P}, m \in \mathcal{M}, t \in \mathcal{T} \quad (3)$$

Eq. 3 constrains the amount of each principal energy type, i.e., that for which F_i is the principal energy output of technology i, that is available during each time period from each continuous-sized technology by its installed capacity.

$$z_{i,kk}^{p,m,t} = \sum_{k \in \mathcal{K}_{I,i}} \frac{y_{i,k}^{p,m,t}}{E_{i,k,kk}}, \forall\ i \in \mathcal{I}, kk \in \mathcal{K}_{O,i}, p \in \mathcal{P}, m \in \mathcal{M}, t \in \mathcal{T} \quad (4)$$

Eq. 4 uses the input energy used by each technology type to determine the amount of energy output produced during each time period.

$$v_\ell^{p,m,t} = \sum_{i \in \mathcal{I}} \sum_{k \in \mathcal{K}_{I,i}} y_{i,k}^{p,m,t} \cdot H_{i,k,\ell} + \sum_{mm \in \mathcal{A}_{k,n}^{p,m,t}} \sum_{n \in \mathcal{N}_{B,P,k}} \sum_{k \in \mathcal{K}} u_{k,n}^{p,m,t,mm} \cdot C_{k,\ell,n},$$
$$\forall\ \ell \in \mathcal{L}, p \in \mathcal{P}, m \in \mathcal{M}, t \in \mathcal{T} \quad (5)$$

Eq. 5 calculates the emission of each type of pollutant as the total of on- and off-site production.

$$e^{p,m,t} = \sum_{mm \in \mathcal{A}_{k,n}^{p,m,t}} \sum_{k \in \mathcal{K}} \left(\sum_{n \in \mathcal{N}_{B,P,k}} u_{k,n}^{p,m,t,mm} \cdot B_{k,n} + \sum_{n \in \left(\mathcal{N}_{B,k} \setminus \mathcal{N}_{B,P,k}\right) \setminus \mathcal{N}_D} u_{k,n}^{p,m,t,mm} \right),$$
$$\forall\ p \in \mathcal{P}, m \in \mathcal{M}, t \in \mathcal{T} \tag{6}$$

Eq. 6 calculates the primary energy not from a fictitious market consumed as the sum of the processed energy of each type and that which is used as an input fuel on site.

$$\sum_{p \in \mathcal{P}} \sum_{m \in \mathcal{M}} \sum_{t \in \mathcal{T}} \sum_{k \in \mathcal{K}} \left(D_k^{p,m,t} + \sum_{mm \in \mathcal{S}_{k,n}^{p,m,t}} \sum_{n \in \mathcal{N}_{S,k}} w_{k,n}^{p,m,t,mm} \right) \geq EF \cdot \sum_{p \in \mathcal{P}} \sum_{m \in \mathcal{M}} \sum_{t \in \mathcal{T}} e^{p,m,t} \tag{7}$$

Eq. 7 implements an energy-efficiency constraint by stating that the ratio of the useful energy consumed as demand and sold off site to the primary energy used and not purchased from a fictitious market must exceed the requirement.

$$r_{k,j}^{p,m,t} = r_{k,j}^{p,m,t-1} \cdot OS_{k,j} + qi_{k,j}^{p,m,t-1} \cdot OI_{k,j} - qo_{k,j}^{p,m,t-1} \cdot OO_{k,j},$$
$$\forall\ k \in \mathcal{K}, j \in \mathcal{J}_S, p \in \mathcal{P}, m \in \mathcal{M}, t \in \mathcal{T} \tag{8}$$

Eq. 8 is an inventory-balance constraint for energy stored in any energy-storage technology: the amount available is equal to the residual level stored in the previous time step plus (or minus) any inflows (or outflows).

$$qo_{k,j}^{p,m,t} \leq OR_{k,j} \cdot r_{k,j}^{p,m,t}, \forall\ k \in \mathcal{K}, j \in \mathcal{J}_S, p \in \mathcal{P}, m \in \mathcal{M}, t \in \mathcal{T} \tag{9}$$

Eq. 9 constrains the amount of energy that may be discharged from any energy-storage technology by the storage level.

$$OA_{k,j} \cdot x_j^p \leq r_{k,j}^{p,m,t} \leq OB_{k,j} \cdot x_j^p, \forall\ k \in \mathcal{K}, j \in \mathcal{J}_S, p \in \mathcal{P}, m \in \mathcal{M}, t \in \mathcal{T} \tag{10}$$

Eq. 10 constrains the amount of energy that may be stored in any energy-storage technology by lower and upper bounds on the installed storage capacity.

2.4 Implementation of Upper-Level Constraints

In this section, we illustrate the logic of the constraints in Section 2.3 at our two test sites, FASAD's Centro de Adultos La Arboleya (in Siero, Asturias, Spain, http://www.fasad.es/index.php?option=com_content&view=article&id=172&Itemid=2) and Fachhochschul Studiengänge Burgenland's Pinkafeld campus (in Pinkafeld, Burgenland, Austria, http://www.fh-burgenland.at/GF/studienorte_pinkafeld.asp). Details on both sites are available from the previous EnRiMa Deliverable D1.1 (HCE et al., 2011). We start with updated Sankey diagrams and collected data for each site. We are then able to draw schemas of energy balances and determine the decision variables using the energy-balance constraints from Section 2.3.

2.4.1 FASAD's Current Installation

Neither passive-measure portfolios nor storage devices are installed. Plus, no forward purchases or sales of energy are made.

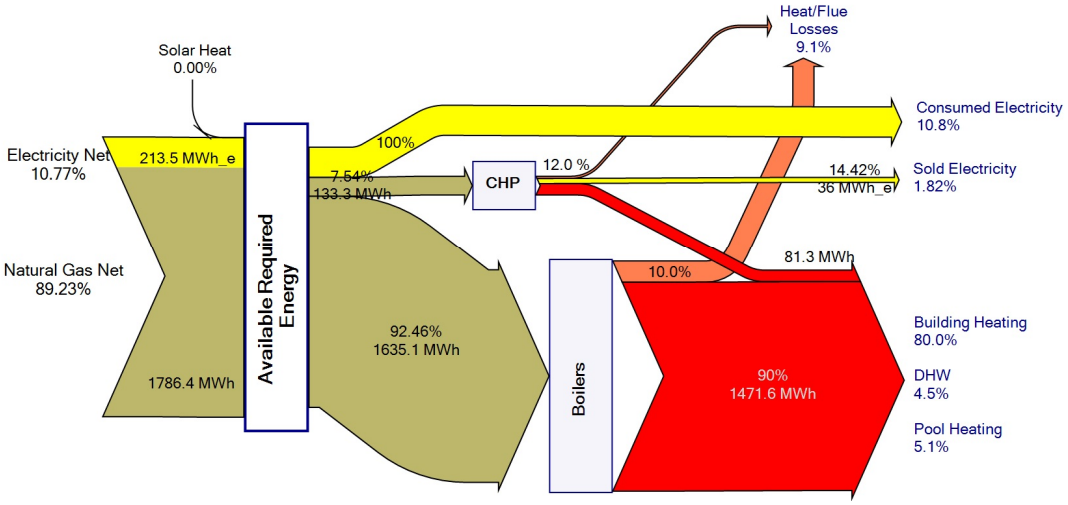

Figure 3: Sankey Diagram for FASAD's Current Installation

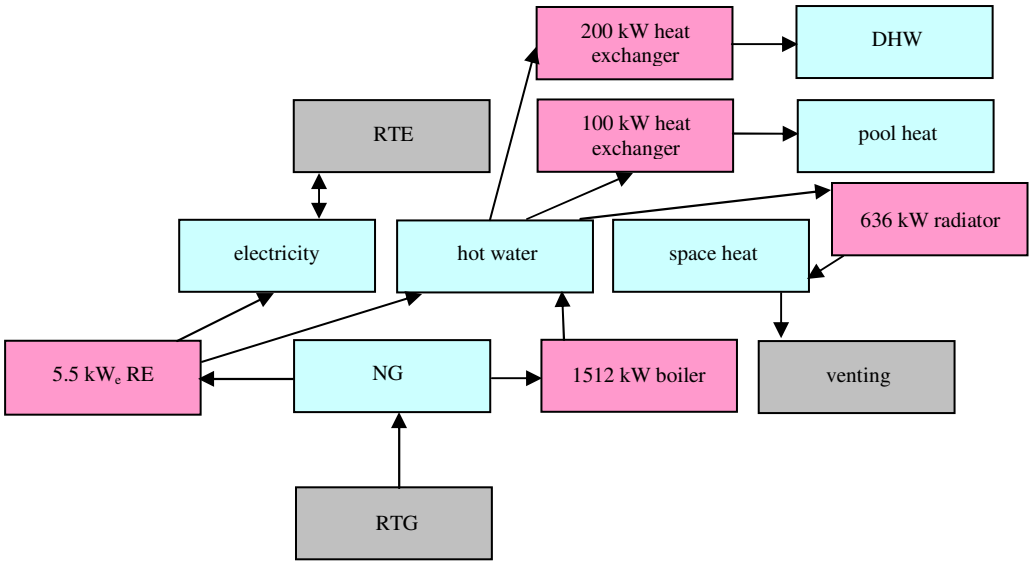

Figure 4: FASAD's Schema of Upper-Level Energy Flows

For the current installation at FASAD (see Figs. 3 and 4) we have the following sets:

- $\mathcal{N}_{E,U} = \{\text{RTE}\}$
- $\mathcal{N}_{G,U} = \{\text{RTG}\}$

- $\mathcal{N}_{S,\text{space heat}} = \{\text{venting}\}$
- $\mathcal{N}_{S,\text{electricity}} = \{\text{RTE}\}$
- $\mathcal{N}_{B,\text{electricity}} = \mathcal{N}_{B,P,\text{electricity}} = \{\text{RTE}\}$
- $\mathcal{N}_{S,\text{NG}} = \{\text{RTG}\}$
- $\mathcal{N}_{B,\text{NG}} = \{\text{RTG}\}$
- $\mathcal{I}_{E,D} = \{5.5\ \text{kW}_e\ \text{RE}\}$
- $\mathcal{I}_{E,C} = \{\emptyset\}$
- $\mathcal{I}_H = \{1512\ \text{kW boiler}, 100\ \text{kW heat exchanger}, 200\ \text{kW heat exchanger}, 636\ \text{kW boiler}\}$
- $\mathcal{I}_C = \{\emptyset\}$
- $\mathcal{J} = \{\emptyset\}$
- $\mathcal{K}_E = \{\text{electricity}\}$
- $\mathcal{K}_H = \{\text{space heat}, \text{hot water}, \text{DHW}, \text{pool heat}\}$
- $\mathcal{K}_C = \{\emptyset\}$
- $\mathcal{K}_G = \{\text{NG}\}$
- $\mathcal{K}_{I,5.5\ \text{kW}_e\ \text{RE}} = \{\text{NG}\}$
- $\mathcal{K}_{I,1512\ \text{kW boiler}} = \{\text{NG}\}$
- $\mathcal{K}_{I,100\ \text{kW heat exchanger}} = \{\text{hot water}\}$
- $\mathcal{K}_{I,200\ \text{kW heat exchanger}} = \{\text{hot water}\}$
- $\mathcal{K}_{I,636\ \text{kW radiator}} = \{\text{hot water}\}$
- $\mathcal{K}_{O,5.5\ \text{kW}_e\ \text{RE}} = \{\text{electricity}, \text{hot water}\}$
- $\mathcal{K}_{O,1512\ \text{kW boiler}} = \{\text{hot water}\}$
- $\mathcal{K}_{O,100\ \text{kW heat exchanger}} = \{\text{pool heat}\}$
- $\mathcal{K}_{O,200\ \text{kW heat exchanger}} = \{\text{DHW}\}$
- $\mathcal{K}_{O,636\ \text{kW radiator}} = \{\text{space heat}\}$
- $\mathcal{L} = \{\text{CO}_2\}$

And the following parameters based on annual data as indicated in HCE et al. (2011) unless otherwise stated are:

- $A^t_{5.5\ \text{kW}_e\ \text{RE}} = 1$
- $A^t_{1512\ \text{kW boiler}} = 1$

- $A^t_{\text{100 kW heat exchanger}} = 1$
- $A^t_{\text{200 kW heat exchanger}} = 1$
- $A^t_{\text{636 kW radiator}} = 1$
- $B_{\text{electricity,RTE}} = 2.0624$ kWh/kWh$_e$ (source: HCE's generation mix in the region of Asturias, http://www.hcenergia.com/en/about-us/generation/asturias)
- $C_{\text{electricity,CO}_2\text{,RTE}} = 0.370$ kg/kWh$_e$
- $D^t_{\text{electricity}} = 213500$ kWh$_e$
- $D^t_{\text{space heat}} = 1386016$ kWh
- $D^t_{\text{DHW}} = 78513$ kWh
- $D^t_{\text{pool heat}} = 88369$ kWh
- $DT = 6500$ hours
- $HO = 1$
- $G_{\text{5.5 kW}_e\text{ RE}} = 5.5$ kW$_e$
- $E_{\text{5.5 kW}_e\text{ RE,NG,electricity}} = 3.7037$ kWh/kWh$_e$
- $E_{\text{5.5 kW}_e\text{ RE,NG,hot water}} = 1.64$ kWh/kWh
- $E_{\text{1512 kW boiler,NG,hot water}} = 1.11$ kWh/kWh
- $E_{\text{100 kW heat exchanger,hot water,pool heat}} = 1$ kWh/kWh
- $E_{\text{200 kW heat exchanger,hot water,DHW}} = 1$ kWh/kWh
- $E_{\text{636 kW radiator,hot water,space heat}} = 1$ kWh/kWh
- $F_{\text{5.5 kW}_e\text{ RE}} = \text{electricity}$
- $F_{\text{1512 kW boiler}} = \text{hot water}$
- $F_{\text{100 kW heat exchanger}} = \text{pool heat}$
- $F_{\text{200 kW heat exchanger}} = \text{DHW}$
- $F_{\text{636 kW radiator}} = \text{space heat}$
- $H_{\text{5.5 kW}_e\text{ RE,NG,CO}_2} = 0.1836$ kg/kWh
- $H_{\text{1512 kW boiler,NG,CO}_2} = 0.1836$ kg/kWh
- $H_{\text{100 kW heat exchanger,hot water,CO}_2} = 0$ kg/kWh
- $H_{\text{200 kW heat exchanger,hot water,CO}_2} = 0$ kg/kWh

- $H_{\text{636 kW radiator,hot water,CO}_2} = 0$ kg/kWh

And the following decision variables:

- $e^t = u^t_{\text{electricity,RTE}} \cdot B_{\text{electricity,RTE}} + u^t_{\text{NG,RTG}} = 440322 + 1768359 = 2208691$ kWh
- $u^t_{\text{electricity,RTE}} = 213500$ kWh$_e$
- $u^t_{\text{NG,RTG}} = 1768359$ kWh
- $v^t_{\text{CO}_2} = y^t_{\text{5.5 kW}_e\text{ RE,NG}} \cdot H_{\text{5.5 kW}_e\text{ RE,NG,CO}_2}$
  $+ y^t_{\text{100 kW heat exchanger,hot water}} \cdot H_{\text{100 kW heat exchanger,hot water,CO}_2}$
  $+ y^t_{\text{200 kW heat exchanger,hot water}} \cdot H_{\text{200 kW heat exchanger,hot water,CO}_2}$
  $+ y^t_{\text{636 kW radiator,hot water}} \cdot H_{\text{636 kW radiator,hot water,CO}_2}$
  $+ y^t_{\text{1512 kW boiler,NG}} \cdot H_{\text{1512 kW boiler,NG,CO}_2}$
  $+ u^t_{\text{electricity,RTE}} \cdot C_{\text{electricity,CO}_2\text{,RTE}} = 24464.7 + 0 + 0 + 0 + 300206.0124 + 78995 = 403665.7124$ kg
- $w^t_{\text{electricity,RTE}} = 35980$ kWh$_e$
- $w^t_{\text{space heat,venting}} = 0$ kWh
- $s^p_{\text{5.5 kW}_e\text{ RE}} = 1$
- $s^p_{\text{1512 kW boiler}} = 1512$ kW
- $s^p_{\text{100 kW heat exchanger}} = 100$ kW
- $s^p_{\text{200 kW heat exchanger}} = 200$ kW
- $s^p_{\text{636 kW radiator}} = 636$ kW
- $y^t_{\text{5.5 kW}_e\text{ RE,NG}} = 133250$ kWh
- $y^t_{\text{1512 kW boiler,NG}} = 1635109$ kWh
- $y^t_{\text{100 kW heat exchanger,hot water}} = 88369$ kWh
- $y^t_{\text{200 kW heat exchanger,hot water}} = 78513$ kWh
- $y^t_{\text{636 kW radiator,hot water}} = 1386016$ kWh
- $z^t_{\text{5.5 kW}_e\text{ RE,electricity}} = 35980$ kWh$_e$
- $z^t_{\text{5.5 kW}_e\text{ RE,hot water}} = 81280$ kWh
- $z^t_{\text{1512 kW boiler,hot water}} = 1471589$ kWh

- $z^t_{\text{100 kW heat exchanger,pool heat}} = 88369$ kWh
- $z^t_{\text{200 kW heat exchanger,DHW}} = 78513$ kWh
- $z^t_{\text{636 kW heat radiator,space heat}} = 1386016$ kWh

The main energy-balance relation, i.e., Eq. 1, can also be shown to be satisfied here using the data for the six types of energy used at FASAD. Keeping in mind that there is neither storage nor forward trading, the energy-balance relation for each energy type is as follows:

- Electricity: $w^t_{\text{electricity,RTE}} + D^t_{\text{electricity}} = z^t_{\text{5.5 kW}_e \text{ RE,electricity}} + u^t_{\text{electricity,RTE}}$, i.e., both sides of the expression equal 249480 kWh_e.
- Space heat: $D^t_{\text{space heat}} = z^t_{\text{636 kW radiator,space heat}}$, i.e., both sides of the expression equal 1386016 kWh.
- DHW: $D^t_{\text{DHW}} = z^t_{\text{200 kW heat exchanger,DHW}}$, i.e., both sides of the expression equal 78513 kWh.
- Hot water: $y^t_{\text{100 kW heat exchanger,hot water}} + y^t_{\text{200 kW heat exchanger,hot water}} + y^t_{\text{636 kW radiator,hot water}} = z^t_{\text{5.5 kW}_e \text{ RE,hot water}} + z^t_{\text{1512 kW boiler,hot water}}$, i.e., both sides of the expression equal 1552869 kWh.
- Pool heat: $D^t_{\text{pool heat}} = z^t_{\text{100 kW heat exchanger,pool heat}}$, i.e., both sides of the expression equal 88369 kWh.
- NG: $y^t_{\text{5.5 kW}_e \text{ RE,NG}} + y^t_{\text{1512 kW boiler,NG}} = u^t_{\text{NG,RTG}}$, i.e., both sides of the expression equal 1768359 kWh.

Using Eq. 7 and the calculated values for e^t and $w^t_{\text{electricity,RTE}}$ along with the data for D^t_k, we find that the overall energy efficiency for the current configuration at FASAD is 81.6%.

2.4.2 Pinkafeld's Current Installation

Similar to FASAD, the Pinkafeld site does not have any passive-measure portfolios or storage devices currently installed. No energy is traded in the forward markets, either.

For the current installation at Pinkafeld (see Figs. 5 and 6 as well as HCE et al. (2011)), we have the following sets:

- $\mathcal{N}_{E,U} = \{\text{RTE}\}$
- $\mathcal{N}_H = \{\text{RTH}\}$
- $\mathcal{N}_D = \{\text{sun}\}$
- $\mathcal{N}_{B,\text{solar}} = \mathcal{N}_{B,P,\text{solar}} = \{\text{sun}\}$
- $\mathcal{N}_{B,\text{hot water}} = \mathcal{N}_{B,P,\text{hot water}} = \{\text{RTH}\}$
- $\mathcal{N}_{B,\text{electricity}} = \mathcal{N}_{B,P,\text{electricity}} = \{\text{RTE}\}$

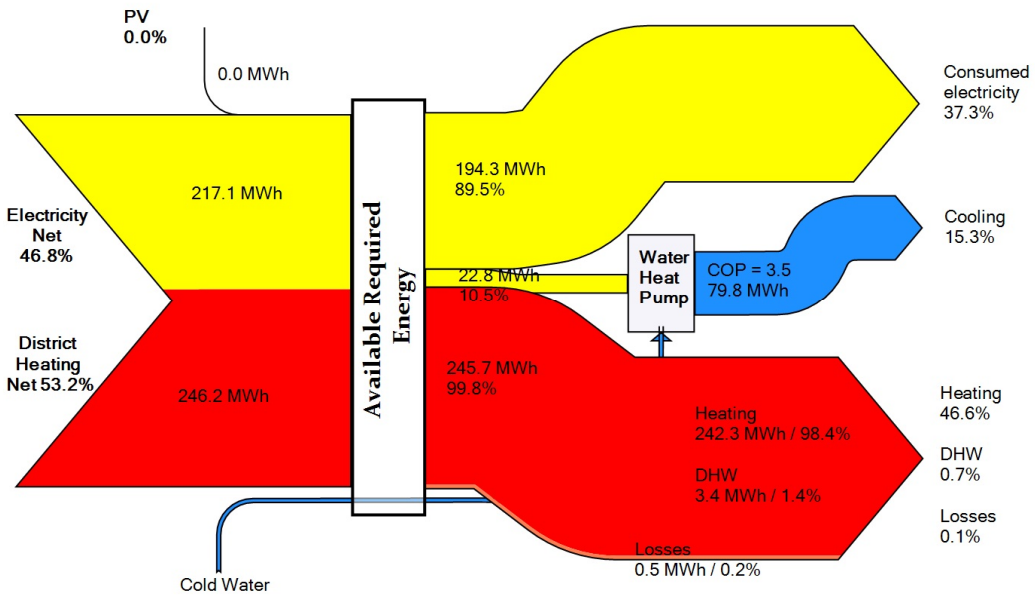

Figure 5: Sankey Diagram for Pinkafeld's Current Installation

- $\mathcal{I}_{E,D} = \{\emptyset\}$
- $\mathcal{I}_{E,C} = \{1.28\ \text{kW}_e\ \text{PV}\}$
- $\mathcal{I}_{H} = \{163\ \text{kW heat exchanger}, 92\ \text{kW radiator}\}$
- $\mathcal{I}_{C} = \{48\ \text{kW heat pump}\}$
- $\mathcal{J} = \{\emptyset\}$
- $\mathcal{K}_{E} = \{\text{electricity}\}$
- $\mathcal{K}_{H} = \{\text{hot water}, \text{space heat}, \text{DHW}\}$
- $\mathcal{K}_{C} = \{\text{cooling}\}$
- $\mathcal{K}_{S} = \{\text{solar}\}$
- $\mathcal{K}_{I,1.28\ \text{kW}_e\ \text{PV}} = \{\text{solar}\}$
- $\mathcal{K}_{O,1.28\ \text{kW}_e\ \text{PV}} = \{\text{electricity}\}$
- $\mathcal{K}_{I,163\ \text{kW heat exchanger}} = \{\text{hot water}\}$
- $\mathcal{K}_{O,163\ \text{kW heat exchanger}} = \{\text{DHW}\}$
- $\mathcal{K}_{I,92\ \text{kW radiator}} = \{\text{DHW}\}$
- $\mathcal{K}_{O,92\ \text{kW radiator}} = \{\text{space heat}\}$
- $\mathcal{K}_{I,48\ \text{kW heat pump}} = \{\text{electricity}\}$
- $\mathcal{K}_{O,48\ \text{kW heat pump}} = \{\text{cooling}\}$

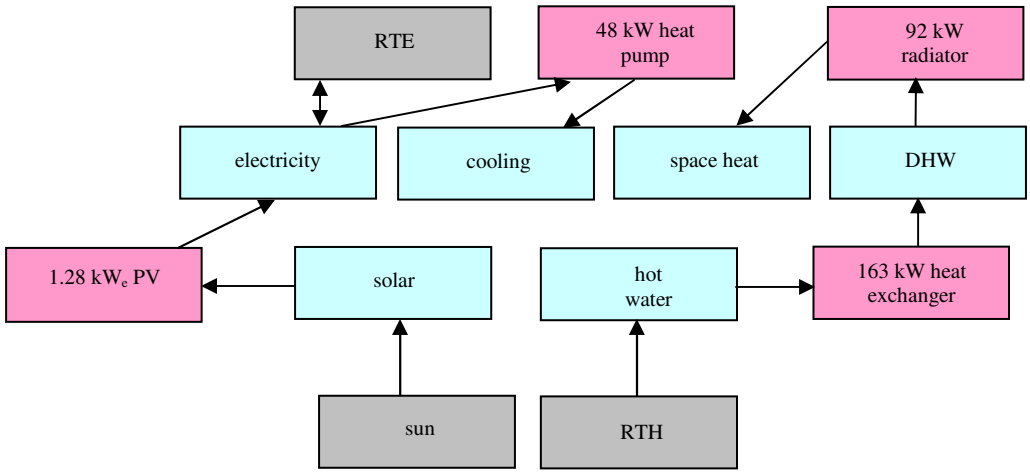

Figure 6: Pinkafeld's Schema of Upper-Level Energy Flows

- $\mathcal{L} = \{\mathrm{CO}_2\}$

And the following parameters:

- $A^t_{\text{1.28 kW}_e\text{ PV}} = 0.5$
- $A^t_{\text{48 kW heat pump}} = 1$
- $A^t_{\text{163 kW heat exchanger}} = 1$
- $A^t_{\text{92 kW radiator}} = 1$
- $B_{\text{solar,sun}} = 0$ kWh/kWh
- $B_{\text{electricity,RTE}} = 1.089$ kWh/kWh$_e$
- $B_{\text{hot water,RTH}} = 2$ kWh/kWh
- $C_{\text{electricity,CO}_2\text{,RTE}} = 0$ kg/kWh$_e$
- $C_{\text{hot water,CO}_2\text{,RTH}} = 0.03$ kg/kWh
- $C_{\text{solar,CO}_2\text{,sun}} = 0$ kg/kWh
- $D^t_{\text{electricity}} = 194273$ kWh$_e$
- $D^t_{\text{cooling}} = 79765$ kWh
- $D^t_{\text{space heat}} = 242290$ kWh
- $D^t_{\text{hot water}} = 0$ kWh
- $D^t_{\text{DHW}} = 3447$ kWh

- $D^t_{\text{solar}} = 0$ kWh
- $E_{1.28\ \text{kW}_e\ \text{PV,solar,electricity}} = 8\ \text{kWh/kWh}_e$
- $E_{163\ \text{kW heat exchanger,hot water,DHW}} = 1.0011\ \text{kWh/kWh}$
- $E_{92\ \text{kW radiator,DHW,space heat}} = 1\ \text{kWh/kWh}$
- $E_{48\ \text{kW heat pump,electricity,cooling}} = 0.2857\ \text{kWh}_e\text{/kWh}$
- $F_{1.28\ \text{kW}_e\ \text{PV}} = \text{electricity}$
- $F_{163\ \text{kW heat exchanger}} = \text{DHW}$
- $F_{92\ \text{kW radiator}} = \text{space heat}$
- $F_{48\ \text{kW heat pump}} = \text{cooling}$
- $H_{1.28\ \text{kW}_e\ \text{PV,solar,CO}_2} = 0\ \text{kg/kWh}$
- $H_{163\ \text{kW heat exchanger,hot water,CO}_2} = 0\ \text{kg/kWh}$
- $H_{92\ \text{kW radiator,DHW,CO}_2} = 0\ \text{kg/kWh}$
- $H_{48\ \text{kW heat pump,electricity,CO}_2} = 0\ \text{kg/kWh}_e$
- $DT = 8760$ hours
- $HO = 1$

And the following decision variables:

- $e^t = u^t_{\text{electricity,RTE}} \cdot B_{\text{electricity,RTE}}$
  $+u^t_{\text{solar,sun}} \cdot B_{\text{solar,run}}$
  $+u^t_{\text{hot water,RTH}} \cdot B_{\text{hot water,RTH}}$
  $= 236381 + 0 + 492460 = 728841$ kWh
- $s^p_{1.28\ \text{kW}_e\ \text{PV}} = 1.28\ \text{kW}_e$
- $s^p_{163\ \text{kW heat exchanger}} = 163$ kW
- $s^p_{92\ \text{kW radiator}} = 92$ kW
- $s^p_{48\ \text{kW heat pump}} = 48$ kW
- $u^t_{\text{electricity,RTE}} = 217063\ \text{kWh}_e$
- $u^t_{\text{hot water,RTH}} = 246230$ kWh
- $u^t_{\text{solar,sun}} = 8$ kWh

- $v^t_{\mathrm{CO_2}} = y^t_{\text{1.28 kW}_e\text{ PV,solar}} \cdot H_{\text{1.28 kW}_e\text{ PV,solar,CO}_2}$
  $+y^t_{\text{163 kW heat exchanger,hot water}} \cdot H_{\text{163 kW heat exchanger,hot water,CO}_2}$
  $+y^t_{\text{92 kW radiator,HWH}} \cdot H_{\text{92 kW radiator,DHW,CO}_2}$
  $+y^t_{\text{48 kW heat pump,electricity}} \cdot H_{\text{48 kW heat pump,electricity,CO}_2}$
  $+u^t_{\text{electricity,RTE}} \cdot C_{\text{electricity,CO}_2\text{,RTE}} + u^t_{\text{solar,sun}} \cdot C_{\text{solar,CO}_2\text{,sun}}$
  $+u^t_{\text{hot water,RTH}} \cdot C_{\text{hot water,CO}_2\text{,RTH}} = 0 + 0 + 0 + 0 + 0 + 0 + 7386.90 = 7386.90$ kg
- $y^t_{\text{1.28 kW}_e\text{ PV,solar}} = 8$ kWh
- $y^t_{\text{163 kW heat exchanger,hot water}} = 246230$ kWh
- $y^t_{\text{92 kW radiator,DHW}} = 242290$ kWh
- $y^t_{\text{48 kW heat pump,electricity}} = 22790$ kWh$_e$
- $w^t_{\text{electricity,RTE}} = 1$ kWh$_e$
- $z^t_{\text{1.28 kW}_e\text{ PV,electricity}} = 1$ kWh$_e$
- $z^t_{\text{163 kW heat exchanger,DHW}} = 245738$ kWh
- $z^t_{\text{92 kW radiator,space heat}} = 242290$ kWh
- $z^t_{\text{48 kW heat pump,cooling}} = 79765$ kWh

As for FASAD, the main energy-balance relation, i.e., Eq. 1, can also be shown to be satisfied here using the data for the six types of energy used at Pinkafeld. Keeping in mind that there is neither storage nor forward trading, the energy-balance relation for each energy type is as follows:

- Electricity: $y^t_{\text{48 kW heat pump,electricity}} + w^t_{\text{electricity,RTE}} + D^t_{\text{electricity}} = z^t_{\text{1.28 kW}_e\text{ PV,electricity}} + u^t_{\text{electricity,RTE}}$, i.e., both sides of the expression equal 218063 kWh$_e$.
- Space heat: $D^t_{\text{space heat}} = z^t_{\text{92 kW radiator,space heat}}$, i.e., both sides of the expression equal 242290 kWh.
- DHW: $y^t_{\text{92 kW radiator,DHW}} + D^t_{\text{DHW}} = z^t_{\text{163 kW heat exchanger,DHW}}$, i.e., both sides of the expression equal 245738 kWh.
- Hot water: $y^t_{\text{163 kW heat exchanger,hot water}} = u^t_{\text{hot water,RTH}}$, i.e., both sides of the expression equal 246230 kWh.
- Cooling: $D^t_{\text{cooling}} = z^t_{\text{48 kW heat pump,cooling}}$, i.e., both sides of the expression equal 79765 kWh.
- Solar: $y^t_{\text{1.28 kW}_e\text{ PV,solar}} = u^t_{\text{solar,sun}}$, i.e., both sides of the expression equal 8 kWh.

Using Eq. 7 and the calculated values for e^t and $w^t_{\text{electricity,RTE}}$ along with the data for D^t_k, we find that the overall energy efficiency for the current configuration at Pinkafeld is 71%.

3 Lower-Level Energy Balance

3.1 Overview

In contrast to Section 2, here, we assume that certain types of end-use energy demands, e.g., for space heat and cooling, are not exogenously given. Rather, the building operator provides acceptable temperature ranges based on user preferences. For example, the end-use demand, $D^{p,m,t}_{\text{space heat}}$, in Eq. 1 may not be fixed and would be determined endogenously. The operational module of the EnRiMa DSS, i.e., for short-term decision making assuming no possibility of changing the building infrastructure or configuration of installed DER, then determines the flow rates of air and water in the conventional heating and HVAC systems that maintain the zone temperature within the specified limits. Consequently, building physics and thermodynamics of both conventional heating and HVAC systems must be reflected as well as the external temperature, solar gain, and internal load. For convenience, we assume that the interior of the building consists of a single zone.

In accordance with EU standards, we use DIN (2003) to model the transfer of heat from the water in the radiator of a conventional heating system to the surrounding air inside the building. Zonal temperature changes are calculated using the method of Platt et al. (2010) for an HVAC system, while the heat exchanged inside a radiator is determined via Xu et al. (2008). The resulting heat demand needed to change the zone temperature to the required one may next be determined based how the conventional heating and HVAC systems are operated. By including these features as constraints in an optimisation model that minimises (expected) energy consumption, energy costs, or CO_2 emissions over a given time horizon, the DSS may provide building operators with a more energy-efficient operating schedule for their installed equipment. We demonstrate our approach's capability by providing preliminary results for the current configurations at our two test sites. This extension to the existing state-of-the-art, i.e., combining optimisation with an accurate representation of building physics and system thermodynamics, is novel and, to our knowledge, exists only in one other working paper, Liang et al. (2011), who focus more on the tradeoff between cost and comfort while abstracting somewhat from the energy flows between the HVAC system and the zone.

Before proceeding to the lower-level constraints and optimisation examples, we first outline the additional nomenclature. As a convention, we use lower-case Greek letters to refer to parameters and upper-case Greek letters to refer to variables (both state and decision) except for those already defined in Section 2, e.g., $D^{p,m,t}_k$ and $y^{p,m,t}_{i,k}$. Thus, the constraints given in Section 3.3 should be considered as supplementing Eqs. 1 through 10 in Section 2.3 by providing richer information for how the $D^{p,m,t}_k$ are determined for end-use energy demands concerning space heat and cooling. As in Section 2, we assume that the constraints are conditional on the current building configuration. Finally, we will suppress the use of indices p and m because operational decisions are more relevant for short-term periods, i.e., made on an hourly basis for a day or a week.

3.2 Nomenclature

3.2.1 Time

- δ: length of operational decision-making period (s)
- η: number of seconds in an hour (s/h)
- $\mathcal{T}_O \subset \mathcal{T}$: set of short-term decision-making periods (see Section 2.2.2)
- t: short-term time period index (see Section 2.2.1)

3.2.2 Physical Constants and Parameters

- γ_{water}: specific heat capacity of water (kJ/(kg·K))
- ρ_{water}: density of water (kg/m^3)
- γ_{air}: specific heat capacity of air (kJ/(kg·K))
- ρ_{air}: density of air (kg/m^3)

3.2.3 Environmental Parameters

- χ^t: external temperature during short-term period $t \in \mathcal{T}_O$ (°C)
- σ^t: fraction of maximum solar insolation incident (weighted average over different wall directions) during short-term period $t \in \mathcal{T}_O$ (kW/m^2)

3.2.4 Building Parameters

- ψ: volume of the zone (m^3)
- ν: heat transition coefficient of the wall (kW/(m^2·K))
- α_{wall}: heat transfer area of the wall (m^2)
- α_{glass}: total area of windows (m^2)
- ϵ: mean energy transmission coefficient of glass (unitless)
- ϕ: mean sun protection factor of all components of the thermal envelope of building (unitless)
- α_{floor}: area of the floor of the zone (m^2)
- λ^t: internal load (from people, lighting, working machines, etc.) per area of the zone during short-term period $t \in \mathcal{T}_O$ (kW/m^2)
- $\underline{\kappa}^t$: lower limit for the required zone temperature during short-term period $t \in \mathcal{T}_O$ (°C)
- $\overline{\kappa}^t$: upper limit for the required zone temperature during short-term period $t \in \mathcal{T}_O$ (°C)

3.2.5 Heating System Parameters

- ζ: supply-water temperature at the radiator inlet (°C)
- ι: maximum amount of heat that can be provided by the conventional heating system in any given short-term time period (kWh)
- $\overline{\mu}_{\text{water}}$ maximum water flow rate in radiator (m^3/s)
- $\underline{\mu}_{\text{water}}$ minimum water flow rate in radiator (m^3/s)
- ξ: mean nominal heat transfer capacity of all radiators installed (kW)
- φ: radiator coefficient (unitless)
- ϱ: mean logarithmic temperature difference (K, which is equivalent to °C since we are referring to a temperature difference)

3.2.6 HVAC System Parameters

- $\overline{\mu}_{\text{vent}}$: maximum air flow rate of the HVAC system (m^3/s)
- $\underline{\mu}_{\text{vent}}$: minimum air flow rate of the HVAC system (m^3/s)
- $\underline{\tau}$: lower limit of the proportion of air that may be taken externally
- $\overline{\tau}$: upper limit of the proportion of air that may be taken externally
- $E_{\text{HVAC,electricity,cooling}}$: electricity required by the HVAC system to produce one unit of cooling (kWh_e/kWh, see Section 2.2.3)
- $E_{\text{boiler,NG,hot water}}$: NG required by the boiler to produce one unit of hot water (kWh/kWh, see Section 2.2.3)
- ω: electricity required to pump the air at a given flow rate ($kWh_e/(m^3/s)$)
- $\overline{\chi}$: external temperature limit at which the AHU performs cooling (°C)
- $\underline{\chi}$: external temperature limit at which the AHU performs heating (°C)
- $\overline{\varsigma}$: AHU's supply-air temperature for heating (°C)
- $\underline{\varsigma}$: AHU's supply-air temperature for cooling (°C)

3.2.7 Energy Market Parameters

- $CP^t_{k,n}$: price of energy type $k \in \mathcal{K}$ purchased from market $n \in \mathcal{N}_{B,k}$ during short-term time period $t \in \mathcal{T}_O$ (€/kWh or €/kWh_e)

3.2.8 State Variables

- Γ^t: return water temperature at the outlet of the radiator during short-term time period $t \in \mathcal{T}_O$ (°C)

3.2.9 Decision Variables

- Λ^t: zone temperature during short-term time period $t \in \mathcal{T}_O$ (°C)
- Ω^t_{water}: flow rate of water to conventional heating system during short-term time period $t \in \mathcal{T}_O$ (m^3/s)
- Ω^t_{vent}: flow rate of air to HVAC system during short-term time period $t \in \mathcal{T}_O$ (m^3/s)
- Υ^t: supply-air temperature from the HVAC system's air-handling unit (AHU) during short-term time period $t \in \mathcal{T}_O$ (°C)
- Φ^t: fraction of external air used by the AHU during short-term time period $t \in \mathcal{T}_O$
- Ψ^t: heat from radiator during short-term time period $t \in \mathcal{T}_O$ (kWh)
- D^t_k: demand for end-use energy type $k = \{\text{space heat}, \text{cooling}\}$ during short-term time period $t \in \mathcal{T}_O$ (kWh, see Section 2.2.3)
- $y^t_{i,k}$: requirement of energy type $k = \{\text{electricity}\}$ as input to energy-creating technology $i = \{\text{HVAC}\}$ during short-term time period $t \in \mathcal{T}_O$ (kWh_e, see Section 2.2.3)

3.3 Constraints

Constraints for the flow of energy at the lower level are described in this section. They should be viewed as supplementing the upper-level constraints in Section 2 by taking a more expansive perspective on certain types of energy demands, building physics, and system thermodynamics. Thus, in line with the EnRiMa DSS schema in Fig. 1, upper- and lower-level energy-balance constraints together would allow the optimisation of operational decisions.

$$\begin{aligned}\Lambda^t \;=\; & \left(\frac{1}{\frac{\gamma_{\text{air}}\cdot\rho_{\text{air}}\cdot\psi}{\delta} + \nu\cdot\alpha_{\text{wall}} + \Omega^t_{\text{vent}}\cdot\rho_{\text{air}}\cdot\gamma_{\text{air}}}\right)\cdot\Bigg[\frac{\gamma_{\text{air}}\cdot\rho_{\text{air}}\cdot\psi}{\delta}\cdot\Lambda^{t-1} \\ & +\Psi^t\cdot\frac{\eta}{\delta} + \nu\cdot\alpha_{\text{wall}}\cdot\chi^{t-1} + \sigma^{t-1}\cdot\epsilon\cdot\phi\cdot\alpha_{\text{glass}} + \lambda^{t-1}\cdot\alpha_{\text{floor}} \\ & +\rho_{\text{air}}\cdot\gamma_{\text{air}}\cdot\Omega^t_{\text{vent}}\cdot\Upsilon^t\Bigg], \forall\, t\in\mathcal{T}_O \end{aligned} \tag{11}$$

Eq. 11 updates the zone temperature based on the current zone temperature, the external temperature, internal load, and both conventional and HVAC systems while accounting for the building shell's characteristics. It is derived from Platt et al. (2010) by adding solar gain and the conventional heating sources. In particular, the terms inside the square brackets on the right-hand side reflect in order the natural zonal temperature change, the heat added by the radiator, the energy lost or gained due to the external temperature, the effect of solar insolation through windows, any internal loads, and heating or cooling via the HVAC system. For clarity, if we consider a simple zone with no heating or HVAC system, then Eq. 11 becomes the following:

$$\Lambda^t = \left(\frac{1}{\frac{\gamma_{\text{air}}\cdot\rho_{\text{air}}\cdot\psi}{\delta}+\nu\cdot\alpha_{\text{wall}}}\right)\cdot\left[\frac{\gamma_{\text{air}}\cdot\rho_{\text{air}}\cdot\psi}{\delta}\cdot\Lambda^{t-1}\right.$$
$$\left.+\nu\cdot\alpha_{\text{wall}}\cdot\chi^{t-1}+\sigma^{t-1}\cdot\epsilon\cdot\phi\cdot\alpha_{\text{glass}}+\lambda^{t-1}\cdot\alpha_{\text{floor}}\right],\forall\, t\in\mathcal{T}_O$$

Thus, according to this simpler equation, the zone temperature in time period t is simply a weighted average of the zone temperature in time period $t-1$, the effect of the external temperature, the effect of solar gain, and the effect of internal load. This approximates the situation in Fig. 7, i.e., that the overall heat flow in the zone must equal the heat transferred through the wall plus the effect of the internal load and solar gain. Eq. 11 is ultimately derived by adding the sources of heating and cooling. The situation for a full conventional heating system is shown in Fig. 8, where the numbers refer to the following:

1. Heat transferred from the radiator to the air
2. Heat from the air ventilation system
3. Heat transferred through the wall connected to the outside
4. Solar gain
5. Internal load

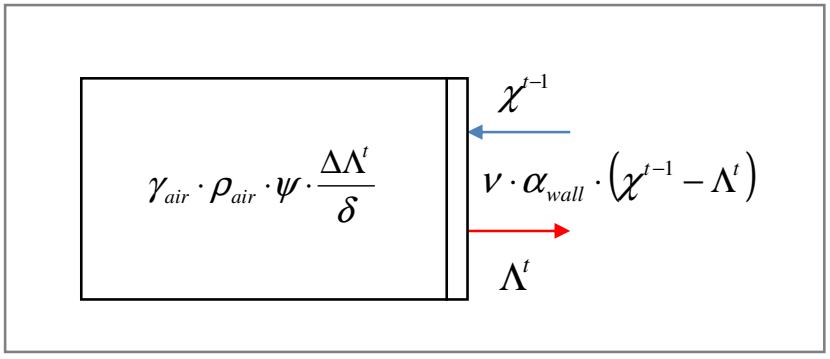

Figure 7: Simple Model with a Wall Separating the Zone from the Outside

$$\underline{\kappa}^t \le \Lambda^t \le \overline{\kappa}^t, \forall\, t\in\mathcal{T}_O \tag{12}$$

Eq. 12 is the constraint on zone temperature, which must be between the lower and upper limits during each short-term time period.

$$\Psi^t = \frac{\delta}{\eta}\cdot\xi\cdot\left(\frac{(\zeta-\Gamma^t)}{\ln\left(\frac{\zeta-\Lambda^t}{\Gamma^t-\Lambda^t}\right)}\cdot\frac{1}{\varrho}\right)^{\varphi},\forall\, t\in\mathcal{T}_O \tag{13}$$

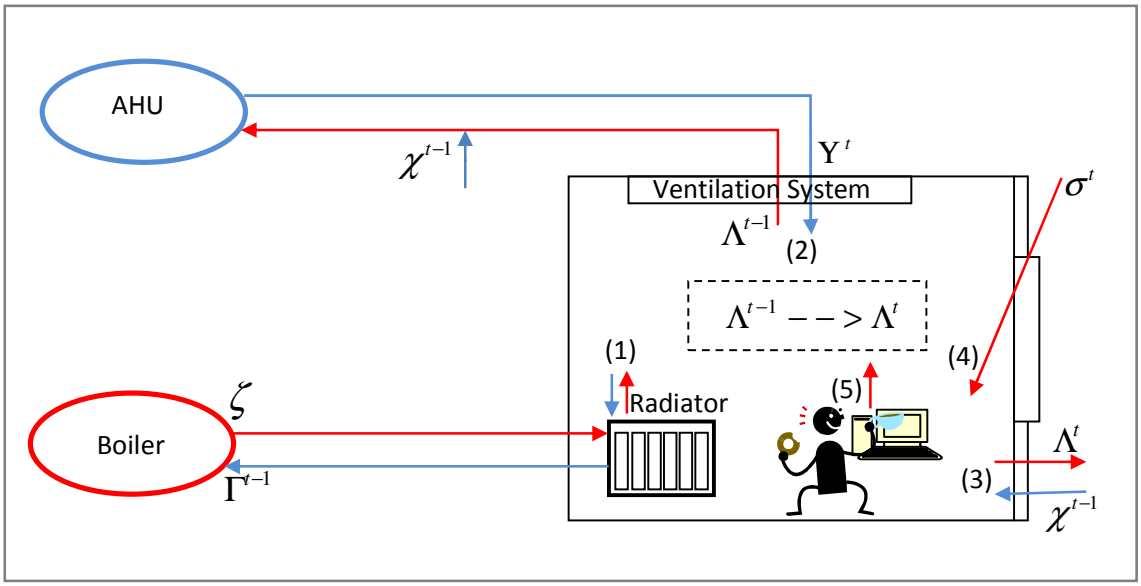

Figure 8: Full Model for the Conventional Heating System

Eq. 13 determines how heat is transferred from the radiator to the air for a conventional heating system. This relationship is derived from DIN (2003) and is dependent on the current zone temperature. Note that φ and ϱ reflect the radiator's technical features. In particular, the former is used to determine the temperature driving force for heat transfer in flow systems. Meanwhile, the latter describes the non-linear relation between the heat output and the mean transmission temperature of the radiator.

$$\Psi^t = \frac{\delta}{\eta} \cdot \Omega^t_{\text{water}} \cdot \rho_{\text{water}} \cdot \gamma_{\text{water}} \cdot \left(\zeta - \Gamma^t\right), \forall\, t \in \mathcal{T}_O \tag{14}$$

Eq. 14 reflects how heat is exchanged inside the radiator and, thus, is a function of the water's flow rate. It is obtained from Xu et al. (2008) assuming that the supply water temperature is constant.

$$D^t_{\text{space heat}} = \frac{\delta}{\eta} \cdot \Omega^t_{\text{water}} \cdot \rho_{\text{water}} \cdot \gamma_{\text{water}} \cdot \left(\zeta - \Gamma^{t-1}\right), \forall\, t \in \mathcal{T}_O \tag{15}$$

Eq. 15 determines the heat required inside the boiler to change the temperature of water from the current return-water temperature to the required supply-water temperature for period.

$$\Lambda^t \leq \Gamma^t \leq \zeta, \forall\, t \in \mathcal{T}_O \tag{16}$$

Eq. 16 states the return-water temperature for each period cannot exceed the supply-water temperature and must be greater than the zone temperature for this period.

$$D^t_{\text{space heat}} \leq \iota, \forall\, t \in \mathcal{T}_O \tag{17}$$

Eq. 17 restricts the maximum heat that can be demanded in any time period.

$$\underline{\mu}_{\text{water}} \leq \Omega^t_{\text{water}} \leq \overline{\mu}_{\text{water}}, \forall\ t \in \mathcal{T}_O \tag{18}$$

Eq. 18 constrains the water flow rate in each period.

$$\Upsilon^t = \begin{cases} \Phi^t \cdot \chi^{t-1} + (1 - \Phi^t) \cdot \Lambda^{t-1} & \text{if ventilation only} \\ \overline{\varsigma} & \text{if cooling and } \chi^{t-1} < \underline{\chi} \\ \overline{\varsigma} + \left(\frac{\underline{\varsigma} - \overline{\varsigma}}{\overline{\chi} - \underline{\chi}}\right) \cdot \left(\chi^{t-1} - \underline{\chi}\right) & \text{if cooling and } \underline{\chi} \leq \chi^{t-1} < \overline{\chi} \\ \underline{\varsigma} & \text{if cooling and } \overline{\chi} \leq \chi^{t-1} \end{cases}, \quad \forall\ t \in \mathcal{T}_O \tag{19}$$

Eq. 19 describes the setting of the supply-air temperature for the AHU, which is a piecewise linear function in case of ventilation with cooling (Engdahl and Johansson, 2004). A stylised representation of the AHU's supply-air temperature as a function of the external temperature is given in Fig. 9. For example, in it, $\overline{\chi} = 20$, $\underline{\chi} = 10$, $\overline{\varsigma} = 18$, and $\underline{\varsigma} = 12$.

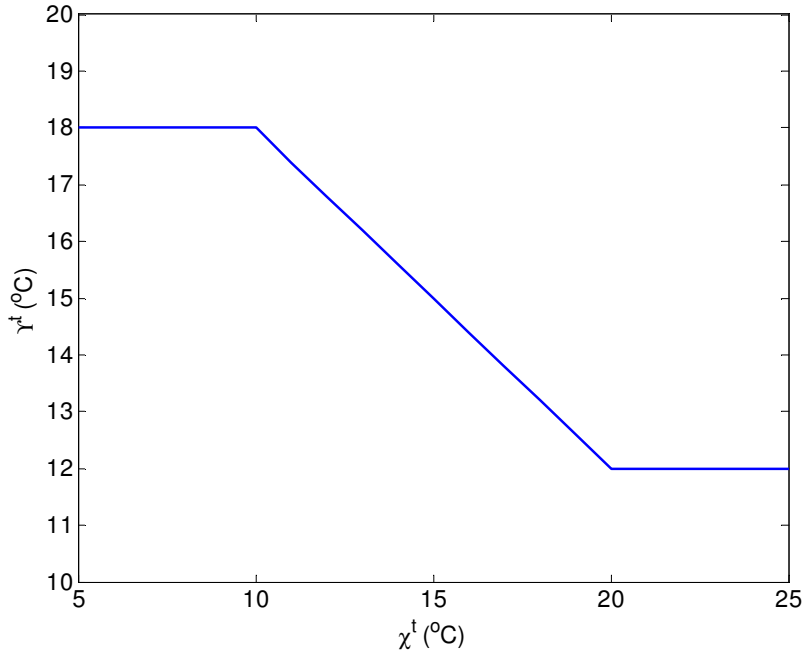

Figure 9: AHU's Stylised Supply-Air Temperature Function

$$D^t_{\text{cooling}} = \Omega^t_{\text{vent}} \cdot \rho_{\text{air}} \cdot \gamma_{\text{air}} \cdot \frac{\delta}{\eta} \cdot \left(\Phi^t \cdot \chi^{t-1} + \left(1 - \Phi^t\right) \cdot \Lambda^{t-1} - \Upsilon^t\right), \forall\ t \in \mathcal{T}_O \tag{20}$$

Eq. 20 calculates the cooling demand for each period as the energy required to bring the temperature of the return air from the AHU mixed with the outside air to the supply-air temperature.

$$y^t_{\text{HVAC,electricity}} = \begin{cases} \omega \cdot \Omega^t_{\text{vent}} & \text{if ventilation only} \\ E_{\text{HVAC,electricity,cooling}} \cdot D^t_{\text{cooling}} & \text{if cooling} \end{cases}, \quad \forall\ t \in \mathcal{T}_O \tag{21}$$

Eq. 21 determines the electricity needed to meet either the ventilation requirement or the cooling demand during each period.

$$\underline{\tau} \leq \Phi^t \leq \overline{\tau}, \forall\ t \in \mathcal{T}_O \tag{22}$$

Eq. 22 constrains the proportion of external air taken in by the AHU during each period.

$$\underline{\mu}_{\text{vent}} \leq \Omega^t_{\text{vent}} \leq \overline{\mu}_{\text{vent}}, \forall\ t \in \mathcal{T}_O \tag{23}$$

Eq. 23 constrains the AHU's air-flow rate during each period.

Given Eqs. 11 through 23, an operational optimisation problem may be formulated for meeting each site's temperature requirements given the existing configuration. These constraints may also be merged with the upper-level constraints from Section 2.3 in order to reflect the site's equipment capacities and financial positions while taking a more expansive view of demand for space heat and cooling, which is being done in the concurrent EnRiMa Deliverable D4.2.

3.4 Implementation of Lower-Level Constraints

In this section, we illustrate the benefits of modelling the operations of the heating and cooling systems via the lower-level constraints described in Section 3.3. Although the upper-level constraints from Section 2.3 may be included (and will be included in the concurrent Deliverable D4.2), here, we focus only on optimising the operations of the heating and cooling systems taking all other operational decisions, e.g., regarding the meeting of other energy requirements, as fixed. Thus, the scope of the optimisation in this section is to determine zonal temperature settings that ultimately result in end-use demand for space heat and cooling (and intermediate electricity demand for the HVAC system) rather than assuming that such demands are fixed. The objective function for a problem covering only the cost minimisation of the conventional heating system for a site such as FASAD that uses a boiler to produce the hot water for space heat (via NG purchased from the RTG market) is:

$$\min \sum_{t \in \mathcal{T}_O} CP^t_{\text{NG,RTG}} \cdot D^t_{\text{space heat}} \cdot E_{\text{boiler,NG,hot water}} \tag{24}$$

On the other hand, if the site is like Pinkafeld, which meets its space heat demand via purchases of district heat from the RTH market and also uses electricity to run an HVAC system, then the objective function that minimises the cost of the energy needed to meet space heat and cooling demands becomes:

$$\min \sum_{t \in \mathcal{T}_O} \left(CP^t_{\text{electricity,RTE}} \cdot y^t_{\text{HVAC,electricity}} + CP^t_{\text{heat,RTH}} \cdot D^t_{\text{space heat}} \right) \tag{25}$$

The objective function in either Eq. 24 or Eq. 25 is subject to the constraints in Eqs. 11 through 23. More elaborate objective functions may be devised and merged with the upper-level operational constraints for a full operational DSS module. However, our aim here is simply to illustrate that the lower-level constraints may be embedded in an optimisation problem that is tractable. Finally, although the examples we present here are on an hourly basis for typical winter days given deterministic energy prices, the model is flexible enough to be run at various time intervals and under uncertain prices, weather conditions, or loads. Furthermore, the objective function may focus on decreasing energy consumption or CO_2 emissions directly.

3.4.1 Numerical Example for FASAD

The parameters along with initial state variables required for FASAD during a typical winter day are indicated below:

- $\delta = 3600$ s
- $\eta = 3600$ s/h
- $\gamma_{\text{water}} = 4.1855$ kJ/(kg·K)
- $\rho_{\text{water}} = 998.2071$ kg/m^3
- $\gamma_{\text{air}} = 1.0189$ kJ/(kg·K)
- $\rho_{\text{air}} = 1.20$ kg/m^3
- $\psi = 41901$ m^3
- $\nu = 0.00133$ kW/(m^2 ·K)
- $\alpha_{\text{wall}} = 2282$ m^2
- $\alpha_{\text{glass}} = 842$ m^2
- $\epsilon = 0.60$
- $\phi = 0.40$
- $\alpha_{\text{floor}} = 5771$ m^2
- $\zeta = 75$ °C
- $\iota = 636$ kWh
- $\overline{\mu}_{\text{water}} = 0.00181$ m^3/s
- $\xi = 636$ kW
- $\Lambda^0 = 16$ °C
- $\Gamma^0 = 50$ °C
- $\overline{\mu}_{\text{vent}} = 10$ m^3/s
- $\underline{\mu}_{\text{vent}} = 0$ m^3/s

- $\varphi = 1.33$
- $\chi^0 = 3.8$ °C
- $\sigma^0 = 0$
- $\lambda^0 = 0.007$ kW/m^2
- $E_{\text{boiler,NG,hot water}} = 1.11$ kWh/kWh
- $CP^t_{\text{electricity,RTE}} = 0.134571$ €/kWh$_e$
- $CP^t_{\text{NG,RTG}} = 0.05056$ €/kWh

In effect, hourly operational decisions are to be made for a full day given deterministic energy prices and accurate weather forecasts for each hour (Table 1).

Table 1: Input Parameter Data for FASAD (Typical Winter Day)

t	χ^t	σ^t	λ^t	$\underline{\kappa}^t$	$\overline{\kappa}^t$
1	3.8	0	0.007	19	22
2	3.5	0	0.007	19	22
3	3.4	0	0.007	19	22
4	3.4	0	0.007	19	22
5	2.9	0	0.007	19	22
6	2.6	0	0.010	19	22
7	2.2	0	0.010	19	22
8	2.2	0	0.010	22	25
9	2.2	0.09248	0.010	22	25
10	2.4	0.12727	0.010	22	25
11	3.1	0.18849	0.010	22	25
12	5.9	0.16171	0.010	22	25
13	6.5	0.17603	0.010	22	25
14	7.0	0.17455	0.010	22	25
15	7.7	0.13605	0.010	22	25
16	8.4	0.12686	0.010	22	25
17	7.7	0	0.010	22	25
18	7.4	0	0.010	22	25
19	6.8	0	0.010	22	25
20	6.4	0	0.010	22	25
21	6.6	0	0.010	22	25
22	5.1	0	0.007	19	22
23	4.8	0	0.007	19	22
24	4.6	0	0.007	19	22

The hourly operational results are given in Tables 2, 3, and 4 for cases with fixed temperature requirements (the mean of the lower and upper desired limits), fixed lower temperature requirements, and a temperature range over which optimisation of the heating and the natural ventilation systems can occur, respectively. The non-linear deterministic optimisation problem for the case with temperature ranges is implemented in Matlab and solved for a typical winter day using hourly decision-making steps within 33 seconds. This optimisation may be performed with shorter decision-making steps, over a longer time horizon, or under uncertain energy prices depending on the user's requirements. These issues will be addressed in the implementation of the EnRiMa DSS in forthcoming WPs.

Daily energy consumption and costs are summarised in Table 5. The optimisation case results in daily energy consumption of 543.81 kWh, which is a 22% reduction from the level of 699.85 kWh in the case where the temperature requirement is set rigidly to the mean of the upper and lower limits. Even when the rigid temperature requirement is set to the lower limit, the total energy consumption is 556.33 kWh, which is 2% higher than in the optimised case with less user comfort. The percentage savings in daily costs are of similar magnitudes. However, these numbers should be treated with caution because of the lack of precision with the parameters available from FASAD used as inputs to the model, e.g., the internal loads or external temperatures. Nevertheless, these are preliminary results simply to illustrate that the lower-level details of the building and heating or cooling systems may be included tractably into an optimisation framework. In subsequent WPs, we will validate the approach using more precise data from both the test site as well as the laboratory facility.

Table 2: Mean-Temperature Lower-Level Operations for FASAD (Typical Winter Day)

t	Λ^t	Υ^t	Ψ^t	Γ^t	Ω^t_{water}	$D^t_{\text{space heat}}$	Ω^t_{vent}
1	20.50	-	108.12	21.39	0.0005	50.41	0
2	20.50	-	44.08	20.52	0.0002	43.37	0
3	20.50	-	45.60	20.52	0.0002	45.60	0
4	20.50	-	46.10	20.52	0.0002	46.10	0
5	20.50	-	46.10	20.52	0.0002	46.10	0
6	20.50	-	48.63	20.53	0.0002	48.64	0
7	20.50	-	32.84	20.50	0.0001	32.82	0
8	23.50	-	92.73	24.14	0.0004	99.36	0
9	23.50	-	50.03	23.54	0.0002	49.45	0
10	23.50	-	31.35	23.50	0.0001	31.32	0
11	23.50	-	23.30	23.50	0.0001	23.30	0
12	23.50	-	7.39	23.50	0.00003	7.39	0
13	23.50	5.90	0.00	23.50	0	0	0.06
14	23.50	6.50	0.00	23.50	0	0	0.35
15	23.50	7.00	0.00	23.50	0	0	0.47
16	23.50	7.70	0.00	23.50	0	0	0.27
17	23.50	8.40	0.00	23.50	0	0	0.38
18	23.50	-	22.21	23.50	0.0001	22.21	0
19	23.50	-	23.73	23.50	0.0001	23.73	0
20	23.50	-	26.77	23.50	0.0001	26.77	0
21	23.50	-	28.79	20.23	0.0001	28.79	0
22	20.50	6.60	0.00	23.50	0	0	1.77
23	20.50	-	37.50	20.51	0.0002	35.44	0
24	20.50	-	39.02	20.51	0.0002	39.02	0

Figs. 10 and 11 indicate how the zone temperatures change during the day relative to the external temperatures. Due to high solar gains in the middle of the day and the rigid temperature requirement, natural ventilation is even required. By contrast, the optimisation case allows the zone temperatures to drift within the acceptable range, thereby taking advantage of the solar gains (Fig. 12).

3.4.2 Numerical Example for Pinkafeld

The parameters along with initial state variables required for Pinkafeld during a typical winter day that are different from those for FASAD are indicated below:

Table 3: Low-Temperature Lower-Level Operations for FASAD (Typical Winter Day)

t	Λ^t	Υ^t	Ψ^t	Γ^t	Ω^t_{water}	$D^t_{\text{space heat}}$	Ω^t_{vent}
1	19.00	3.80	79.18	19.25	0.0003	35.51	0
2	19.00	3.80	36.49	19.00	0.0002	36.63	0
3	19.00	3.50	38.01	19.00	0.0002	38.01	0
4	19.00	3.40	38.51	19.00	0.0002	38.51	0
5	19.00	3.40	38.51	19.00	0.0002	38.51	0
6	19.00	2.90	41.04	19.01	0.0002	41.05	0
7	19.00	2.60	25.25	19.00	0.0001	25.24	0
8	22.00	2.20	85.14	22.42	0.0004	90.68	0
9	22.00	2.20	42.45	22.01	0.0002	42.12	0
10	22.00	2.20	23.76	22.00	0.0001	23.75	0
11	22.00	2.40	15.72	22.00	0.0001	15.72	0
12	22.00	3.10	0.00	22.00	0	0	0.01
13	22.00	5.90	0.00	22.00	0	0	0.45
14	22.00	6.50	0.00	22.00	0	0	0.78
15	22.00	7.00	0.00	22.00	0	0	0.93
16	22.00	7.70	0.00	22.00	0	0	0.74
17	22.00	8.40	0.00	22.00	0	0	0.88
18	22.00	7.70	14.63	22.00	0.0001	14.63	0
19	22.00	7.40	16.14	22.00	0.0001	16.14	0
20	22.00	6.80	19.18	22.00	0.0001	19.18	0
21	22.00	6.40	21.20	22.00	0.0001	21.20	0
22	19.00	6.60	0.00	22.00	0	0	2.49
23	19.00	5.10	29.92	19.00	0.0001	28.31	0
24	19.00	4.80	31.43	19.00	0.0001	31.43	0

- $\psi = 11081.104$ m^3
- $\nu = 0.000413$ kW/(m^2 $\cdot$K)
- $\alpha_{\text{wall}} = 6143$ m^2
- $\alpha_{\text{glass}} = 426$ m^2
- $\phi = 0.670118$
- $\alpha_{\text{floor}} = 2088.8825$ m^2
- $\zeta = 80$ °C
- $\iota = 168$ kWh
- $\overline{\mu}_{\text{water}} = 0.00245$ m^3/s
- $\xi = 168$ kW
- $\Gamma^0 = 40$ °C
- $\overline{\mu}_{\text{vent}} = 3.61$ m^3/s
- $\varphi = 1.33$
- $\chi^0 = -3.56$ °C

Table 4: Optimal Lower-Level Operations for FASAD (Typical Winter Day)

t	Λ^t	Υ^t	Ψ^t	Γ^t	Ω^t_{water}	$D^t_{\text{space heat}}$	Ω^t_{vent}
1	20.26	-	103.53	21.02	0.0005	47.95	0
2	19.30	-	24.29	19.30	0.0001	23.54	0
3	19.00	-	33.75	19.00	0.0001	33.58	0
4	19.00	-	38.51	19.00	0.0002	38.52	0
5	19.00	-	38.51	19.00	0.0002	38.51	0
6	19.00	-	41.04	19.01	0.0002	41.05	0
7	19.00	-	25.25	19.00	0.0001	25.24	0
8	22.00	-	85.14	22.42	0.0004	90.68	0
9	22.00	-	42.45	22.01	0.0002	42.12	0
10	22.00	-	23.76	22.00	0.0001	23.75	0
11	24.42	-	62.48	24.57	0.0003	65.66	0
12	23.80	-	0.00	24.57	0	0	0
13	23.79	-	0.00	24.57	0	0	0
14	24.09	-	0.00	24.57	0	0	0
15	24.43	-	0.00	24.57	0	0	0
16	24.46	-	0.00	24.57	0	0	0
17	24.57	-	0.00	24.57	0	0	0
18	23.14	-	0.00	24.57	0	0	0
19	22.00	-	0.00	24.57	0	0	0
20	22.00	-	19.15	22.00	0.0001	18.22	0
21	22.04	-	21.89	22.04	0.0001	21.91	0
22	20.98	-	0.00	22.04	0	0	0
23	19.00	-	1.74	19.00	0	1.65	0
24	19.00	-	31.43	19.00	0.0001	31.43	0

Table 5: Summary of Lower-Level Operational Results for FASAD (Typical Winter Day)

Case	Space Heat Demand (kWh)	Cost (€)
Fixed Mean Temperature	699.85	39.28
Fixed Lower Temperature	556.33	31.22
Optimisation with Fixed Prices	543.81	30.52

- $\lambda^0 = 0.001436$ kW/m^2
- $\underline{\tau} = 0$
- $\overline{\tau} = 0.50$
- $E_{\text{HVAC,electricity,cooling}} = 0.2857$ kWh$_e$/kWh
- $\overline{\varsigma} = 18$ °C
- $\underline{\varsigma} = 12$ °C
- $\overline{\chi} = 20$ °C
- $\underline{\chi} = 10$ °C
- $CP^t_{\text{electricity,RTE}} = 0.15$ €/kWh$_e$
- $CP^t_{\text{heat,RTH}} = 0.08028$ €/kWh

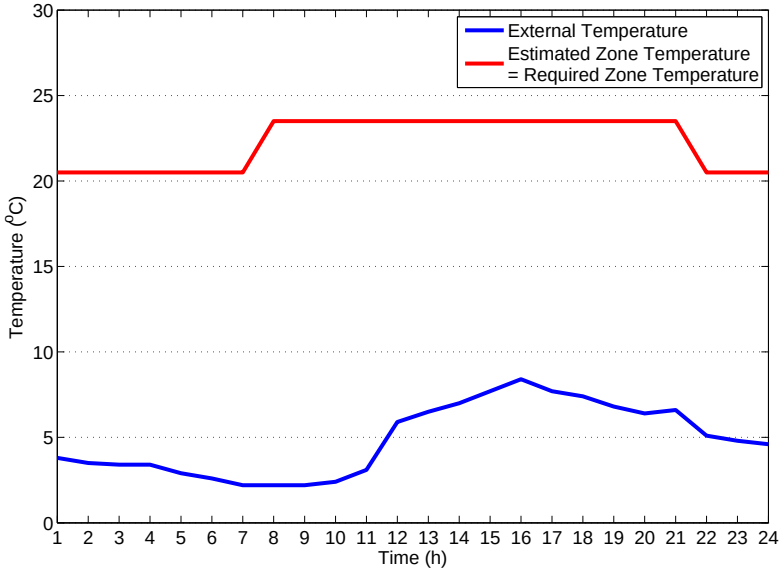

Figure 10: Mean Fixed-Temperature Setting for FASAD (Typical Winter Day)

- $\omega = 0.75$ kWh$_e$/(m^3/s)

Again, hourly operational decisions are to be made during each hour for a full day. Besides the fixed energy prices, we also perform a case with a TOU tariff for both electricity and heat prices as in Table 6.

The hourly operational results for fixed prices (the current situation for Pinkafeld) are given in Tables 7, 8, and 9 for the same three cases as for FASAD in Section 3.4.1. In addition, since Pinkafeld has an HVAC system, the fraction of external air that can be taken in by the AHU is 0.50 in the two cases with fixed temperature requirements, whereas it is a decision variable in the optimisation case. However, this has a minor impact on the overall results due to the relatively low electricity requirements. Optimisation results under a TOU tariff (a possibility in the future) are given in Table 10. The non-linear deterministic optimisation problems for the two cases with temperature ranges are again solved in Matlab using hourly decision-making steps within 33 seconds.

Daily energy consumption and costs are summarised in Table 11. The optimisation case results in daily energy consumption of 632.79 kWh (or 632.84 kWh under a TOU tariff), which is a 10% reduction from the level of 701.84 in the case where the temperature requirement is set rigidly to the mean of the upper and lower limits. Unlike the example for FASAD in Section 3.4.1, we could be more confident in the preliminary results for Pinkafeld due to the availability of more precise data. Again, when the rigid temperature requirement is set to the lower limit, the total energy consumption is 638.78 kWh, which is 1% higher than in the optimised case with less user comfort. Hence, the optimisation approach proposed here may support building operators in trading off energy costs and user comfort.

Figs. 13 and 14 indicate how the zone temperatures change during the day relative to the external temperatures. Due to high solar gains in the middle of the day and the rigid temperature requirement, the HVAC system needs to be operated, which creates relatively high electricity consumption in comparison to the two optimisation cases. By contrast, the two optimisation cases again allow the zone temperatures to drift within the acceptable

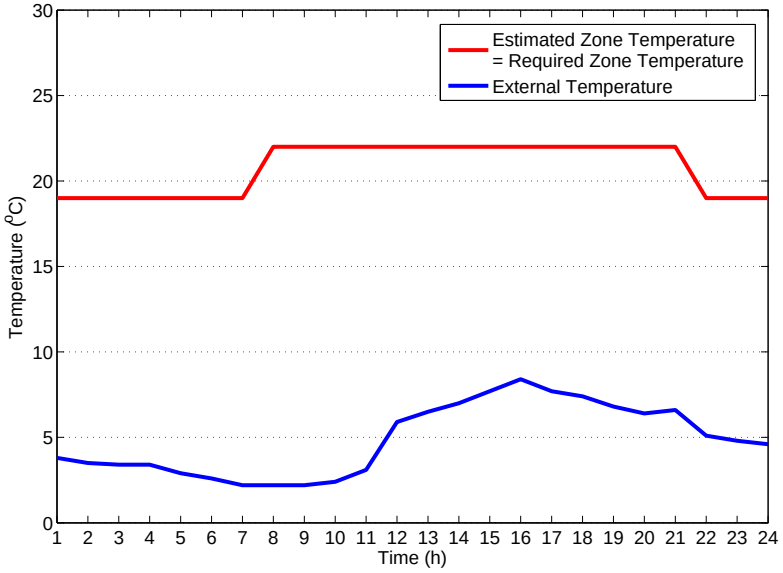

Figure 11: Low Fixed-Temperature Setting for FASAD (Typical Winter Day)

range, thereby taking advantage of the solar gains (Figs. 15 and 16). While the pattern of energy consumption is similar, the case with a TOU tariff results in pre-heating of the building at 6 AM. Given the temperature range, the operational module of the DSS is able to keep the zone temperature within the range by taking advantage of the solar gain during the late afternoon hours. The daily space heat demand is 629.15 kWh and 629.24 kWh with fixed prices and a TOU tariff, respectively. In addition, there is 3.64 kWh_e of electricity required in each case for ventilation as opposed to 5.77 kWh_e and 7.77 kWh_e in the cases with fixed required temperatures. Surprisingly, even with a lower fixed temperature setting as in Table 8 and Fig. 14, the energy and cost savings are not as high as with an optimisation that provides a temperature range. In effect, the flexibility of the building's conventional heating and HVAC systems to respond to environmental and market conditions is valuable from both economic and energy-efficiency perspectives.

4 Conclusions

Improving energy efficiency in public buildings is a critical component of the EU's policy for reaching its climate target goals for 2020, i.e., reduction by 20% of the total energy consumption, 20% contribution of renewable energies to total energy production, and 20% reduction of greenhouse gases such as CO_2 below 1990 emissions. The EnRiMa project will provide an ICT-based DSS with enhancements to the existing state-of-the-art research in terms of modelling energy flows, generating scenarios for dealing with uncertainties, and developing an SMS to handle multi-criteria stochastic optimisation at the building level. In this document, the first of these features is the focus as we create a flexible approach for modelling energy flows that could be applicable to nearly any EU public building. The advantage of such an approach is that the resulting energy-balance relations are set based and may be implemented as constraints in an optimisation (the focus of the SMS in Deliverable D4.2). We use the data collected for our two test sites in order to illustrate how the energy

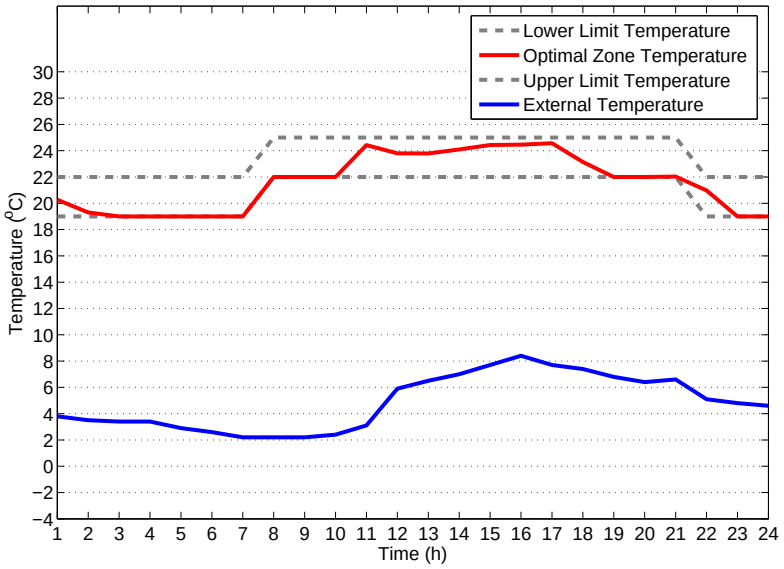

Figure 12: Optimal Zone Temperatures for FASAD (Typical Winter Day)

flows may be modelled at both the upper level, i.e., assuming fixed end-use energy demands and disregarding both building physics and system thermodynamics, and the lower level, i.e., abstracting from strategic decisions and focusing on the operation of conventional heating and HVAC systems. At the upper level, we demonstrate how the principal energy-balance relation is satisfied, while we run a partial operational optimisation at the lower level to yield preliminary results, which are encouraging because they imply that energy consumption and cost may be reduced by 10% from simply deploying the existing energy resources more efficiently.

It should be strongly emphasised that these numerical results are preliminary and are done in order to illustrate that our approach of merging building physics with an optimisation perspective is tractable and potentially beneficial to building operators. At the moment, we do not have accurate enough data, viz., about internal loads and external temperatures, for the FASAD site in order to have results that are consistent with observations. However, the results for Pinkafeld are more in concordance with observations, and we will validate the model in future WPs in order to make it a suitable component of the final DSS.

Overall, this deliverable meets Operational Objective O1 of the EnRiMa DoW as follows:

1. Energy-balance relations that link energy resources to loads at each decision-making step in order to specify the efficiency of each alternative.

2. Energy-transfer constraints that determine the capacity of each resource that will be available based on existing capacities, amount of recoverable heat, and state of charge, for example.

3. The incorporation of the impact of building retrofits on energy flows is included in the upper-level energy-balance constraints of Section 2.3 and explained fully in Appendix B.

4. The development of lower-level energy-balance constraints in Section 3.3 that take user comfort, building physics, and system thermodynamics into consideration.

Table 6: Input Parameter Data for Pinkafeld (Typical Winter Day)

t	χ^t	σ^t	λ^t	$\underline{\kappa}^t$	$\overline{\kappa}^t$	$CP^t_{\text{electricity,RTE}}$	$CP^t_{\text{heat,RTH}}$
1	-3.6	0	0.00287	16	17	0.15	0.06
2	-3.1	0	0.00287	16	17	0.15	0.06
3	-2.8	0	0.00287	16	17	0.15	0.06
4	-2.5	0	0.00287	16	17	0.15	0.06
5	-2.1	0	0.00287	16	17	0.15	0.06
6	-2.0	0	0.00287	16	17	0.15	0.06
7	-1.7	0	0.00287	19	22	0.20	0.10
8	-1.8	0	0.00287	19	22	0.20	0.10
9	-1.4	0.075329	0.006885	19	22	0.20	0.10
10	-0.4	0.140061	0.009935	19	22	0.20	0.10
11	0.6	0.150898	0.010329	19	22	0.20	0.10
12	1.5	0.184557	0.010902	19	22	0.20	0.10
13	2.6	0.169501	0.010455	19	22	0.20	0.10
14	3.4	0.229950	0.013456	19	22	0.20	0.10
15	3.6	0.240787	0.014351	19	22	0.20	0.10
16	3.0	0.197716	0.013028	19	22	0.20	0.10
17	1.8	0	0.00287	19	22	0.20	0.10
18	1.7	0	0.00287	18	22	0.20	0.10
19	2.6	0	0.00287	16	17	0.17	0.08
20	1.4	0	0.00287	16	17	0.17	0.08
21	0.7	0	0.00287	16	17	0.17	0.08
22	0.6	0	0.00287	16	17	0.17	0.08
23	0.6	0	0.00287	16	17	0.17	0.08
24	0.2	0	0.00287	16	17	0.17	0.08

5. An automated procedure for calculating energy-transfer efficiencies is explained in Appendix A and illustrated via an example for a back-up site.

6. A survey of the literature in Appendix C to demonstrate that part-load efficiency is not relevant for the technologies we consider at the building level. Nevertheless, we provide a stylised formulation to deal with this feature in case it is encountered in future work.

For future work, the energy-balance constraints developed in this deliverable will be used in subsequent WP 4 tasks, viz., 4.5 through 4.7. There, the stochastic optimisation for both the strategic and operational modules will be implemented and tested. There is also a strong link with WPs 5 and 6 as the DSS will have to be installed and validated at our two test sites. Finally, WP 7 will perform a recovery-of-investment analysis in order to quantify the benefits of the EnRiMa DSS and to propose an exploitation plan in order to increase impact for stakeholders in the EU. Finally, a working paper based on Section 3 is to be submitted to either the *IEEE Transactions on Power Systems* or *Computational Management Science* after having been presented at the Computational Management Science Conference (London, 18–20 April) and the EURO Conference (Vilnius, 8–11 July).

Acknowledgements

This document was prepared jointly by EnRiMa partners UCL, IIASA, CET, SINTEF, Tecnalia, and HCE. Quality control was done by Tecnalia (internal reviewer) and URJC (external reviewer). Comments received from SU and MCC have also improved the work.

Table 7: Mean-Temperature Lower-Level Operations for Pinkafeld (Typical Winter Day with Fixed Prices)

t	Λ^t	Φ^t	Υ^t	Ψ^t	Γ^t	Ω^t_{water}	$D^t_{\text{space heat}}$	Ω^t_{vent}	$y^t_{\text{HVAC,electricity}}$
1	16.50	0.00	-	49.78	26.74	0.0002	37.38	0	0
2	16.50	0.00	-	44.99	24.73	0.0002	43.36	0	0
3	16.50	0.00	-	43.73	24.23	0.0002	43.33	0	0
4	16.50	0.00	-	42.97	23.93	0.0002	42.74	0	0
5	16.50	0.00	-	42.20	23.63	0.0002	41.98	0	0
6	16.50	0.00	-	41.19	23.25	0.0002	40.91	0	0
7	20.50	0.00	-	66.14	40.38	0.0004	94.74	0	0
8	20.50	0.00	-	50.32	32.24	0.0003	41.75	0	0
9	20.50	0.00	-	50.58	32.36	0.0003	50.70	0	0
10	20.50	0.00	-	28.28	23.59	0.0001	23.88	0	0
11	20.50	0.00	-	8.28	20.52	0	7.85	0	0
12	20.50	0.00	-	3.06	20.50	0	3.06	0	0
13	20.50	0.50	11.00	0.00	20.50	0	0	0.5322	0.40
14	20.50	0.50	11.55	0.00	20.50	0	0	0.4989	0.37
15	20.50	0.50	11.95	0.00	20.50	0	0	2.3065	1.73
16	20.50	0.50	12.05	0.00	20.50	0	0	2.7435	2.06
17	20.50	0.50	11.75	0.00	20.50	0	0	1.5593	1.17
18	20.00	0.00	-	38.29	26.41	0.0002	42.52	0	0
19	16.50	0.00	-	18.38	17.17	0.0001	15.67	0	0
20	16.50	0.00	-	29.27	19.37	0.0001	30.33	0	0
21	16.50	0.00	-	32.31	20.23	0.0001	32.78	0	0
22	16.50	0.00	-	34.09	20.78	0.0001	34.40	0	0
23	16.50	0.00	-	34.34	20.86	0.0001	34.39	0	0
24	16.50	0.00	-	34.34	20.86	0.0001	34.34	0	0

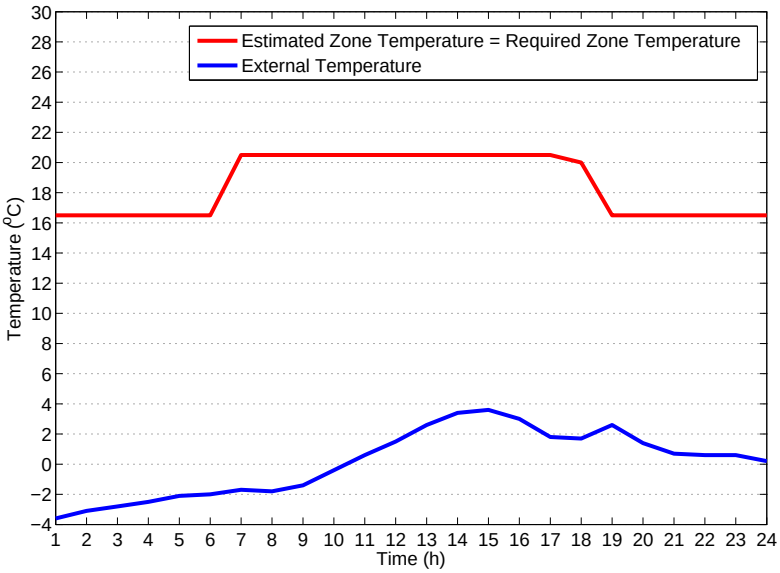

Figure 13: Mean Fixed-Temperature Setting for Pinkafeld (Typical Winter Day with Fixed Prices)

Table 8: Low-Temperature Lower-Level Operations for Pinkafeld (Typical Winter Day with Fixed Prices)

t	Λ^t	Φ^t	Υ^t	Ψ^t	Γ^t	Ω^t_{water}	$D^t_{\text{space heat}}$	Ω^t_{vent}	$y^t_{\text{HVAC,electricity}}$
1	16.00	0.00	-	46.62	24.77	0.0002	33.77	0	0
2	16.00	0.00	-	43.73	23.61	0.0002	42.83	0	0
3	16.00	0.00	-	42.46	23.12	0.0002	42.09	0	0
4	16.00	0.00	-	41.70	22.83	0.0002	41.49	0	0
5	16.00	0.00	-	40.94	22.55	0.0002	40.73	0	0
6	16.00	0.00	-	39.92	22.17	0.0002	39.66	0	0
7	19.00	0.00	-	58.57	34.23	0.0003	74.00	0	0
8	19.00	0.00	-	46.52	28.54	0.0002	41.38	0	0
9	19.00	0.00	-	46.77	28.66	0.0002	46.87	0	0
10	19.00	0.00	-	24.47	20.93	0.0001	21.27	0	0
11	19.00	0.00	-	4.48	19.00	0	4.33	0	0
12	19.00	0.50	9.80	0.00	19.00	0	0	0.0659	0.05
13	19.00	0.50	10.25	0.00	19.00	0	0	0.9335	0.70
14	19.00	0.50	10.80	0.00	19.00	0	0	0.9241	0.69
15	19.00	0.50	11.20	0.00	19.00	0	0	2.9274	2.20
16	19.00	0.50	11.30	0.00	19.00	0	0	3.4149	2.56
17	19.00	0.50	11.00	0.00	19.00	0	0	2.0945	1.57
18	18.00	0.00	-	21.24	19.19	0.0001	21.31	0	0
19	16.00	0.00	-	22.75	17.34	0.0001	22.08	0	0
20	16.00	0.00	-	28.00	18.49	0.0001	28.52	0	0
21	16.00	0.00	-	31.04	19.30	0.0001	31.46	0	0
22	16.00	0.00	-	32.82	19.81	0.0001	33.10	0	0
23	16.00	0.00	-	33.07	19.89	0.0001	33.11	0	0
24	16.00	0.00	-	33.07	19.89	0.0001	33.07	0	0

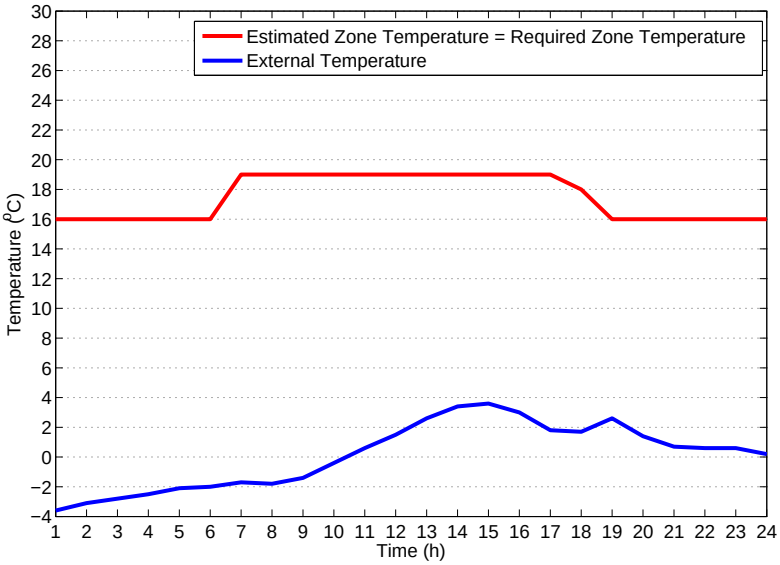

Figure 14: Low Fixed-Temperature Setting for Pinkafeld (Typical Winter Day with Fixed Prices)

Table 9: Optimal Lower-Level Operations for Pinkafeld (Typical Winter Day with Fixed Prices)

t	Λ^t	Φ^t	Υ^t	Ψ^t	Γ^t	Ω^t_{water}	$D^t_{\text{space heat}}$	Ω^t_{vent}	$y^t_{\text{HVAC,electricity}}$
1	16.00	0.00	-	46.62	24.77	0.0002	33.77	0	0
2	16.00	0.00	-	43.73	23.61	0.0002	42.83	0	0
3	16.00	0.00	-	42.46	23.12	0.0002	42.09	0	0
4	16.00	0.00	-	41.70	22.83	0.0002	41.49	0	0
5	16.00	0.00	-	40.94	22.55	0.0002	40.73	0	0
6	16.74	0.00	-	44.60	24.88	0.0002	46.48	0	0
7	19.00	0.00	-	55.78	32.84	0.0003	65.20	0	0
8	19.00	0.00	-	46.52	28.54	0.0002	42.63	0	0
9	19.00	0.00	-	46.77	28.66	0.0002	46.87	0	0
10	19.00	0.00	-	24.47	20.93	0.0001	21.27	0	0
11	19.00	0.00	-	4.48	19.00	0	4.33	0	0
12	19.12	0.00	-	0.00	19.00	0	0	0	0
13	20.66	0.00	-	0.00	19.00	0	0	0	0
14	21.46	0.00	-	0.00	19.00	0	0	0	0
15	22.00	0.50	12.43	0.00	19.00	0	0	1.5615	1.17
16	22.00	0.50	12.80	0.00	19.00	0	0	2.1815	1.64
17	22.00	0.50	12.50	0.00	19.00	0	0	1.1086	0.83
18	18.00	0.00	-	20.05	18.99	0.0001	20.04	0	0
19	16.00	0.00	-	22.75	17.34	0.0001	22.15	0	0
20	16.00	0.00	-	28.00	18.49	0.0001	28.52	0	0
21	16.00	0.00	-	31.04	19.30	0.0001	31.46	0	0
22	16.00	0.00	-	32.82	19.81	0.0001	33.10	0	0
23	16.00	0.00	-	33.07	19.89	0.0001	33.11	0	0
24	16.00	0.00	-	33.07	19.89	0.0001	33.07	0	0

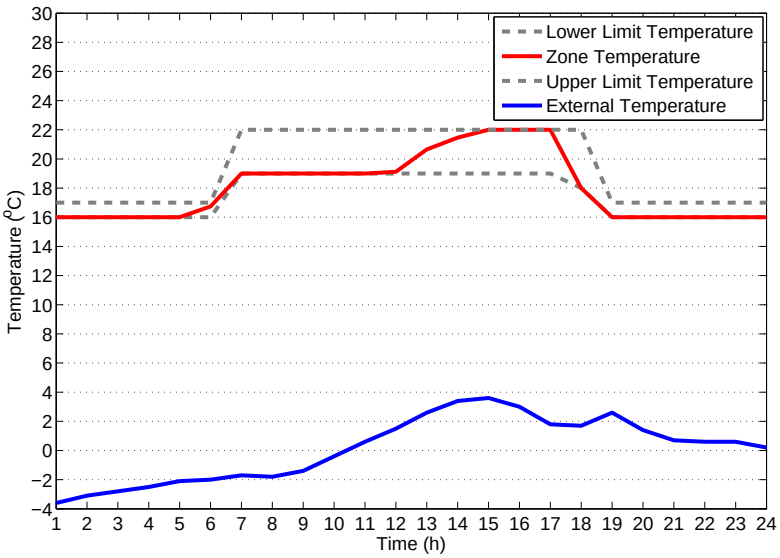

Figure 15: Optimal Zone Temperatures for Pinkafeld (Typical Winter Day with Fixed Prices)

Table 10: Optimal Lower-Level Operations for Pinkafeld (Typical Winter Day with a TOU Tariff)

t	Λ^t	Φ^t	Υ^t	Ψ^t	Γ^t	Ω^t_{water}	$D^t_{\text{space heat}}$	Ω^t_{vent}	$y^t_{\text{HVAC,electricity}}$
1	16.00	0.00	-	46.62	24.77	0.0002	33.77	0	0
2	16.00	0.00	-	43.73	23.61	0.0002	42.83	0	0
3	16.00	0.00	-	42.46	23.12	0.0002	42.09	0	0
4	16.00	0.00	-	41.70	22.83	0.0002	41.49	0	0
5	16.00	0.00	-	40.94	22.55	0.0002	40.73	0	0
6	17.00	0.00	-	46.22	25.87	0.0002	49.06	0	0
7	19.00	0.00	-	54.81	32.37	0.0003	62.29	0	0
8	19.00	0.00	-	46.52	28.54	0.0002	43.06	0	0
9	19.00	0.00	-	46.77	28.66	0.0002	46.87	0	0
10	19.00	0.00	-	24.47	20.93	0.0001	21.27	0	0
11	19.00	0.00	-	4.48	19.00	0	4.33	0	0
12	19.12	0.00	-	0.00	19.00	0	0	0	0
13	20.66	0.00	-	0.00	19.00	0	0	0	0
14	21.46	0.00	-	0.00	19.00	0	0	0	0
15	22.00	0.50	12.43	0.00	19.00	0	0	1.5615	1.17
16	22.00	0.50	12.80	0.00	19.00	0	0	2.1815	1.64
17	22.00	0.50	12.50	0.00	19.00	0	0	1.1086	0.83
18	18.00	0.00	-	20.05	18.99	0.0001	20.04	0	0
19	16.00	0.00	-	22.75	17.34	0.0001	22.15	0	0
20	16.00	0.00	-	28.00	18.49	0.0001	28.52	0	0
21	16.00	0.00	-	31.04	19.30	0.0001	31.46	0	0
22	16.00	0.00	-	32.82	19.81	0.0001	33.10	0	0
23	16.00	0.00	-	33.07	19.89	0.0001	33.11	0	0
24	16.00	0.00	-	33.07	19.89	0.0001	33.07	0	0

Table 11: Summary of Lower-Level Operational Results for Pinkafeld (Typical Winter Day)

Case	Space Heat Demand (kWh)	HVAC Electricity Demand (kWh_e)	Cost (€)
Fixed Mean Temperature	696.11	5.77	56.74
Fixed Lower Temperature	631.01	7.77	51.83
Optimisation with Fixed Prices	629.15	3.64	51.05
Optimisation with a TOU Tariff	629.24	3.64	50.41

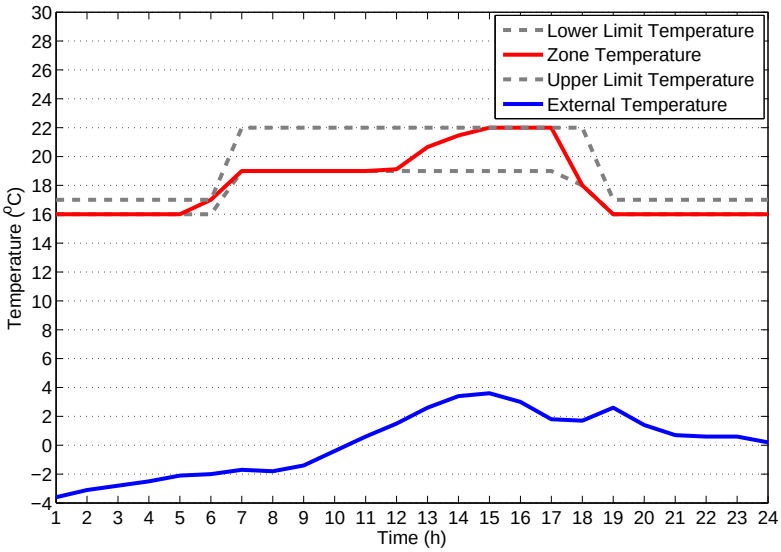

Figure 16: Optimal Zone Temperatures for Pinkafeld (Typical Winter Day with a TOU Tariff)

References

Bonilla, A., E. Cagigal, A. Mediavilla, E. Perea, J. Pérez, A. Romero, and E. Turienzo (2008). Auzener: Modelo de Simulación Virtual del Balance Energético de Barrios Orientado a la Optimización Energética y Económica de los Mismos. In *II Jornadas de Investigación en Construcción*. Instituto de Ciencias de la Construcción Eduardo Torroja, CSIC, Madrid, Spain.

Conejo, A., M. Carrión, and J. Morales (2010). *Decision Making under Uncertainty in Electricity Markets*. Heidelberg, Germany: Springer.

DIN (2003). Heizkörper und Konvektoren - Teil 1: Technische Spezifikationen und Anforderungen. National Standard DIN EN 442-1, Deutsches Institut für Normung e.V.

DIN (2006). Wärmeschutz und Energie-Einsparung in Gebäuden - Wärmebrücken - Planungs- und Ausführungsbeispiele. National Standard DIN 4108 Beiblatt 2, Deutsches Institut für Normung e.V.

DIN (2007). Energetische Bewertung von Gebäuden - Berechnung des Nutz-, End- und Primärenergiebedarfs für Heizung, Kühlung, Lüftung, Trinkwarmwasser und Beleuchtung - Teil 2: Nutzenergiebedarf für Heizen und Kühlen von Gebäudezonen. National Standard DIN V 18599-2, Deutsches Institut für Normung e.V.

DIN (2008). Energieeffizienz von Gebäuden - Berechnung des Energiebedarfs für Heizung und Kühlung. National Standard DIN EN ISO 13790, Deutsches Institut für Normung e.V.

Engdahl, F. and D. Johansson (2004). Optimal Supply Air Temperature with Respect to Energy Use in a Variable Air Volume System. *Energy and Buildings 36*(3), 205–218.

Groissböck, M., M. Stadler, T. Edlinger, A. Siddiqui, S. Heydari, and E. Perea (2011). The First Step for Implementing a Stochastic-based Energy Management System at Campus Pinkafeld. Technical Report C-2011-1, Center for Energy and Innovative Technologies.

HCE, IIASA, SU, UCL, URJC, SINTEF, CET, and Tecnalia (2011). Requirement Assessment. EnRiMa Deliverable D1.1, European Commission FP7 Project Number 260041.

Hobbs, B. (1995). Optimization Methods for Electric Utility Resource Planning. *European Journal of Operational Research 83*(1), 1–20.

IIASA, SU, UCL, URJC, SINTEF, CET, HCE, and Tecnalia (2011). Requirement Analysis. EnRiMa Deliverable D4.1, European Commission FP7 Project Number 260041.

Kaarsberg, T., R. Fiskum, A. Deppe, S. Kumar, A. Rosenfeld, J. Romm, and L. Gielen (2000). Combined Heat and Power for Saving Energy and Carbon in Residential Buildings. In *2000 ACEEE Summer Study on Energy Efficiency in Buildings - Proceedings*. American Council for an Energy Efficient Economy, Washington, D.C., U.S.A.

King, D. and M. Morgan (2007). Adaptive-Focused Assessment of Electric Power Microgrids. *Journal of Energy Engineering 133*(3), 150–164.

Liang, Y., D. Levine, and Z.-J. Shen (2011). Thermostats for the SmartGrid: Models, Benchmarks, and Insights. Working paper, University of California Energy Institute.

Marnay, C., G. Venkataramanan, M. Stadler, A. Siddiqui, R. Firestone, and B. Chandran (2008). Optimal Technology Selection and Operation of Commercial-Building Microgrids. *IEEE Transactions on Power Systems 23*(3), 975–982.

Matic, J. (2007). *Betriebliche Modellierung, Auslegung und Management von dezentralen Energiesystemen*. Ph. D. thesis, Universität Duisburg-Essen, Essen, Germany.

Platt, G., J. Li, R. Li, G. Poulton, G. James, and J. Wall (2010). Adaptive HVAC Zone Modeling for Sustainable Buildings. *Energy and Buildings 42*, 412–421.

Rahman, S. and M. Pipattanasomporn (2010). Modeling and Simulation of a Distributed Generation-Integrated Intelligent Microgrid. Technical Report Strategic Environmental Research and Development Program SERDP Project SI-1650, Advanced Research Institute, Virginia Tech, Arlington, V.A., U.S.A.

UCL, CET, HCE, and Tecnalia (2011). Sankey Diagrams that Link the Energy Resources to the Loads. EnRiMa Deliverable D2.1, European Commission FP7 Project Number 260041.

Winston, W. and M. Venkataramanan (2002). *Introduction to Mathematical Programming: Applications and Algorithms*. Andover, Hampshire, U.K.: Cengage Learning.

Xu, B., L. Fu, and H. Di (2008). Dynamic Simulation of Space Heating Systems with Radiators Controlled by TRVs in Buildings. *Energy and Buildings 40*, 1755–1764.

Appendix A: Procedure for Creating Sankey Diagrams

A Sankey diagram is a graphical tool that is used to illustrate the flow of energy between processes. In particular, the width of the arrows is proportional to the size of the energy flow. Part of EnRiMa's progress beyond the state-of-the-art is to automate the calculation of the energy-transfer efficiencies used in creating Sankey diagrams. The Website of one EnRiMa partner, CET, presents the daily Sankey diagram of a back-up site, ENERGYbase, in Vienna, Austria. The Webpage, http://www.cet.or.at/enrima/sankey_en.php, shows the functionality of the file transfer from a potential test site to the partner's Web server. The transferred file includes the daily energy consumption and weather details, which are stored at 15-minute intervals. In the background, a daily job collects the energy flow details of the day and stores them into a Microsoft (MS) Excel file. This file is processed into a Sankey diagram, which can be chosen here to check the daily energy flows at ENERGYbase.

The sequence of actions (see Fig. 17) is as follows:

- At the test site, data are collected and stored continuously within the building management system (BMS). This back-up test site uses DESIGO from Siemens.
- With the help of the BMS, a pre-defined set of data is stored within the MS Excel file "data.xls."
- Each day at the building operator's computer, an MS Windows script (cmd) is executed to transfer the collected data (*.xls file) to the pre-defined FTP server (renaming the file to "dd.mm.yyyy.hh.ii.xls").

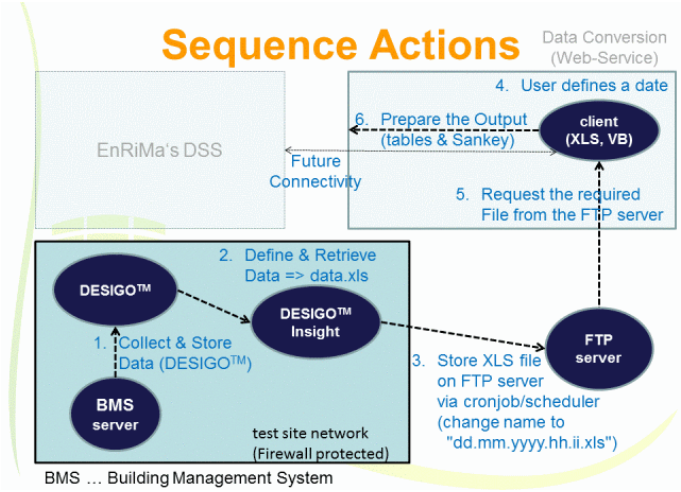

Figure 17: General Data-Collecting sequence for EnRiMa Test Sites

- Each day at the building operator's computer, an MS Windows script (cmd) is executed to convert these collected data into a figure (Sankey), which is uploaded it to the pre-defined FTP server as well.

The Sankey diagram in Fig. 18 represents the daily energy flows at ENERGYbase. Energy flows are displayed via a Sankey diagram, thereby allowing users to track electrical and thermal energy flows from their supply up to their final utilisation. Yellow lines represent electricity flows, while red lines represent heat flows within the Sankey diagram. All numbers are given in kWh and indicate overall daily energy flows. This Sankey diagram is constructed using data collected in Figs. 19 through 21, i.e., the monthly energy demand from December 2011 to February 2012, inclusive, at ENERGYbase, which are inputs for the energy-transfer efficiencies, $E_{i,k,kk}$, of Section 2.2.3.

Appendix B: Treatment of Passive Measures

Here, we demonstrate how the LoadCalc tool developed by CET (Groissböck et al., 2011) may be used to estimate the effects of passive measures such as changes to the building's envelope. By considering representative portfolios of passive measures, we are able to estimate the percentage decrease in the end-use energy consumption of type $k \in \mathcal{K}$ due to each portfolio type $j \in \mathcal{J}_P$ for a given building configuration. In other words, using the procedure of this appendix, we estimate the parameters $OD_{k,j}$ that are defined in Section 2.2.3 and used in Eq. 1. These parameters may be used as an input to the optimisation problem that the strategic EnRiMa DSS solves. For example, we would require a matrix in the form of Table 12. Only ten possible portfolios are indicated here, but any reasonable number could be proposed depending on the interests of the building manager. Here, portfolio 1 is the most modest one with 10% and 12.5% reductions in the demand for space heat and cooling, respectively, relative to the building's current consumption. By contrast, portfolio 10 is the most ambitious one with 60% and 70% reductions, respectively. It is also possible that adoption of a passive measure may reduce heating demand while increasing that of

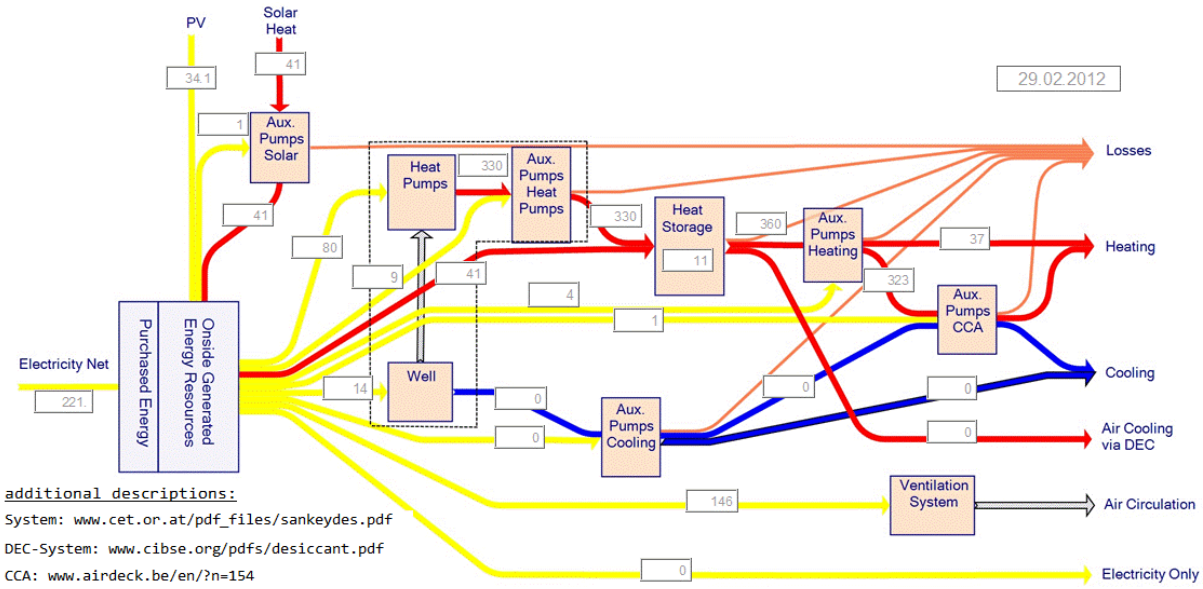

Figure 18: Sankey Diagram for ENERGYbase (29 February 2012)

cooling. Of course, investment costs of each portfolio may also be obtained and used as input parameters to the optimisation problem solved by the strategic module of the EnRiMa DSS. The details of this are in the concurrent Deliverable D4.2. Representative costs of these portfolios may start at €10k (for the most modest one) and be as high as €500k (for the most ambitious one) depending on the nature of the portfolios and the building's current configuration. How these portfolios are adopted is beyond the scope of this deliverable and is, rather, a topic for the SMS in the concurrent Deliverable D4.2 and future deliverables to consider. Instead, we outline here how CET's LoadCalc tool uses information about the building's existing configuration in order to estimate the $OD_{k,j}$ parameters.

The LoadCalc tool determines the end-use energy consumption for space heat and cooling for a given building configuration depending on the building's shell, solar gains, internal

Data for Sankey Diagram December 2011											
	I_{mean}	74.58 W/m²	T_{mean}	2.98 °C							
			IN			OUT					
IN total	kWh	$\%_{in,total}$	kWh_{el}	kWh_{th}	Process	kWh_{el}	kWh_{th}	OUT total	kWh_{el}	kWh_{th}	$\%_{th}$
electricity net	9944.1	60.6	994.0	---	well	---	0.0	heating	0.0	30030.0	100.0
PV	2591.9	15.8	6974.0		heat pumps	---	27400.0	cooling	0.0	0.0	0.0
solar heat	3885.0	23.7	601.0	27400.0	aux. pumps heat pumps	---	27400.0	electricity only	0.0	0.0	0.0
			---	31285.0	heat storage Puffer + Solar	---	30030.0	DEC-System	0.0	0.0	0.0
			32.0	3885.0	aux. pumps solar heat	---	3885.0				
			10.0	0.0	aux. pumps cooling	---	0.0				
			122.0	30030.0	aux. pumps heating	---	30030.0				
			3679.0	---	ventilation system	---	---				
			124.0	22768.0	aux. pumps CCA	---	22768.0			Heating	
				0.0			0.0			Cooling	
sum	16421.0	100.0	12536.0		sum	0.0		sum	0.0	30030.0	

Figure 19: Data for Sankey Diagram at ENERGYbase (December 2011)

Data for Sankey Diagram January 2012

I_{mean} 74.58 W/m² T_{mean} 2.98 °C

			IN			OUT					
IN total	kWh	$\%_{in,total}$	kWh_{el}	kWh_{th}	Process	kWh_{el}	kWh_{th}	OUT total	kWh_{el}	kWh_{th}	$\%_{th}$
electricity net	9944.1	60.6	994.0	—	well	—	0.0	heating	0.0	30030.0	100.0
PV	2591.9	15.8	6974.0		heat pumps	—	27400.0	cooling	0.0	0.0	0.0
solar heat	3885.0	23.7	601.0	27400.0	aux. pumps heat pumps	—	27400.0	electricity only	0.0	0.0	0.0
			—	31285.0	heat storage Puffer + Solar	—	30030.0	DEC-System	0.0	0.0	0.0
			32.0	3885.0	aux. pumps solar heat	—	3885.0				
			10.0	0.0	aux. pumps cooling	—	0.0				
			122.0	30030.0	aux. pumps heating	—	30030.0				
			3679.0	—	ventilation system	—	—				
			124.0	22768.0	aux. pumps CCA	—	22768.0				
				0.0			0.0				
sum	16421.0	100.0	12536.0		sum	0.0		sum	0.0	30030.0	

Heating
Cooling

Figure 20: Data for Sankey Diagram at ENERGYbase (January 2012)

Data for Sankey Diagram February 2012

I_{mean} 115.11 W/m² T_{mean} -1.74 °C

			IN			OUT					
IN total	kWh	$\%_{in,total}$	kWh_{el}	kWh_{th}	Process	kWh_{el}	kWh_{th}	OUT total	kWh_{el}	kWh_{th}	$\%_{th}$
electricity net	10708.1	53.3	1187.0	—	well	—	0.0	heating	0.0	38080.0	99.8
PV	3775.9	18.8	8539.0		heat pumps	—	34630.0	cooling	0.0	0.0	0.0
solar heat	5624.0	28.0	885.0	34630.0	aux. pumps heat pumps	—	34630.0	electricity only	0.0	0.0	0.0
			—	40254.0	heat storage Puffer + Solar	—	38080.0	DEC-System	0.0	80.0	0.2
			44.0	5624.0	aux. pumps solar heat	—	5624.0				
			9.0	0.0	aux. pumps cooling	—	0.0				
			128.0	38080.0	aux. pumps heating	—	38080.0				
			3582.0	—	ventilation system	—	—				
			110.0	27912.0	aux. pumps CCA	—	27912.0				
				0.0			0.0				
sum	20108.0	100.0	14484.0		sum	0.0		sum	0.0	38160.0	

Heating
Cooling

Figure 21: Data for Sankey Diagram at ENERGYbase (February 2012)

loads, infiltration, and thermal heat transfer. When the same end-use energy consumption is calculated under a modified building configuration that installs the retrofits proposed by any one of the portfolios of passive measures, the percentage change in the end-use energy demand of each type may be calculated. Thus, these serve as estimates of the $OD_{k,j}$ parameters. Fig. 22 indicates the various forces that interact to determine the zone temperature. These may include thermal heat transfer (based on the difference between the external and internal surface temperatures), external gains (mainly through windows), internal gains (such as loads from occupants or electrical equipment), effects of heating or

Table 12: Energy-Reducing Effects of Representative Portfolios of Passive Measures

j	$OD_{\text{space heat},j}$	$OD_{\text{cooling},j}$
1	0.10	0.125
2	0.15	0.25
⋮	⋮	⋮
10	0.60	0.70

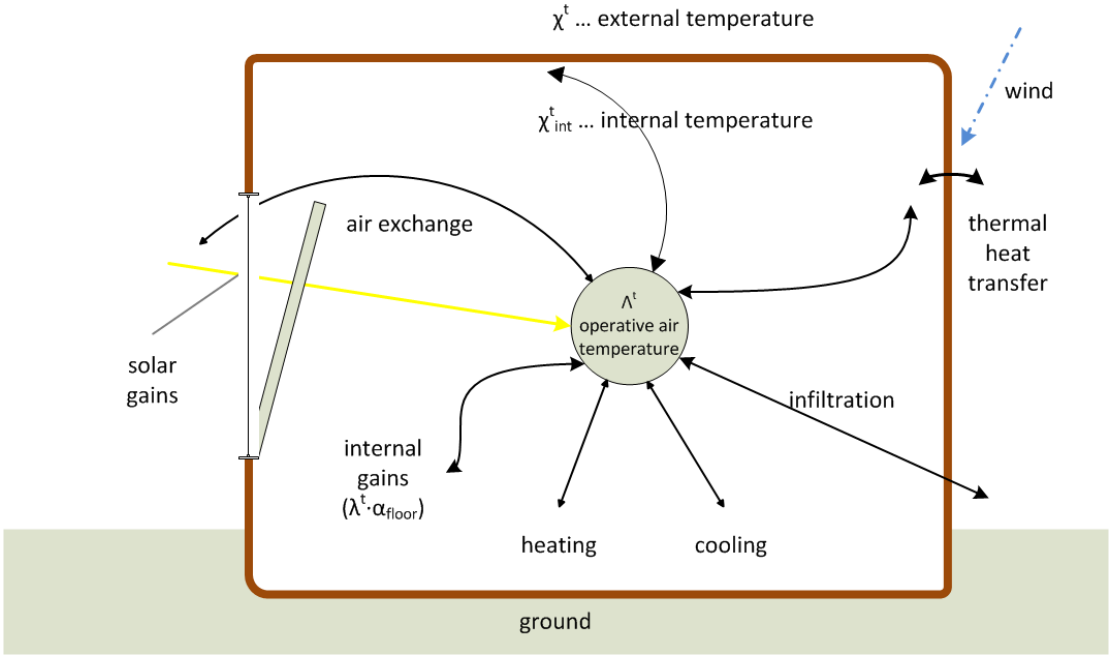

Figure 22: Energy-Flow Paths within a Building

cooling systems, and natural infiltration. We summarise these effects via Eq. 26 as follows:

$$\Xi^t = \left(\sum_{d \in \mathcal{D}_O} \varpi_d^t + \sum_{d \in \mathcal{D}_T} \varpi_d^t + \lambda^t \cdot \alpha_{\text{floor}} + \sum_{d \in \mathcal{D}_I} \varpi_d^t + \sum_{d \in \mathcal{D}_A} \varpi_d^t \right) \cdot \frac{\delta}{\eta}, \forall\, t \in \mathcal{T} \qquad (26)$$

The nomenclature associated with this equation is as follows:

- d: index for type of energy flow
- $\mathcal{D} \supset \mathcal{D}_O \cup \mathcal{D}_T \cup \mathcal{D}_I \cup \mathcal{D}_A$: set of all types of energy flows
  - $\mathcal{D}_O$: set of energy flows across opaque surfaces
  - $\mathcal{D}_T$: set of energy flows through transparent surfaces
  - $\mathcal{D}_I$: set of energy flows through natural infiltration
  - $\mathcal{D}_A$: set of energy flows through the air
- Ξ^t: total heat flow during period $t \in \mathcal{T}$, i.e., a negative (positive) value requires cooling (heating) (kWh)
- ϖ_d^t: heat exchange during period $t \in \mathcal{T}$ involving surface type $d \in \mathcal{D}$ (kW)
- λ^t: internal load per area of the zone during period $t \in \mathcal{T}$ (kW/m^2)
- α_{floor}: area of the floor of the zone (m^2)
- δ: length of decision-making period (s)
- η: number of second in an hour (s/h)

Next, each component of Eq. 26 may be derived separately. First, we explore losses through opaque surfaces (DIN, 2006):

$$\varpi_d^t = (FF_d \cdot \nu_d \cdot \alpha_d + \nu\nu_d \cdot \alpha_d) \cdot \left(\Lambda^t - \chi^t\right), \forall\ t \in \mathcal{T}, d \in \mathcal{D}_O \quad (27)$$

The additional nomenclature associated with this equation is as follows:

- FF_d: temperature correction coefficient for surface type $d \in \mathcal{D}_O$, e.g., 1.0 for the outer wall and 0.6 for the floor next to the soil
- ν_d: heat transition coefficient of surface $d \in \mathcal{D}_O$, i.e., a lower one implies greater efficiency (kW/m^2 ·K)
- α_d: area of the surface (m^2)
- $\nu\nu_d$: thermal coupling coefficient, which corrects for losses through corners (kW/m^2 ·K)
- Λ^t: zone temperature during period $t \in \mathcal{T}$

Eq. 27 accounts for losses through opaque surfaces like walls. It also corrects for the heat losses through thermal bridges, e.g., corners, via the $\nu\nu_d$ terms. In particular, if $\nu_d \leq 0.0004$, then $\nu\nu_d = 0.0001$, but if $0.0004 \leq \nu_d < 0.0008$, then $\nu\nu_d = 0.00005$. Finally, if $\nu_d \geq 0.0008$, then $\nu\nu_d = 0$ (DIN, 2008).

Second, we explore losses through transparent surfaces:

$$\varpi_d^t = (FF_d \cdot (\nu_d - \theta_d \cdot \epsilon \cdot FF_d) \cdot \alpha_d + \nu\nu_d \cdot \alpha_d) \cdot \left(\Lambda^t - \chi^t\right), \forall\ t \in \mathcal{T}, d \in \mathcal{D}_T \quad (28)$$

The additional nomenclature associated with this equation is as follows:

- θ_d: direction correction coefficient, e.g., 0.00095 for north, 0.00165 for both east and west, and 0.00240 for south (kW/m^2 ·K)
- ϵ: mean energy transmission coefficient of glass

The parameter FF_d for glass is 1.00 without any sun protection, decreases to 0.75 with a reflecting surface, and goes all the way down to 0.25 with externally mounted blinds.

As for internal loads, i.e., $\lambda^t \cdot \alpha_{\text{floor}}$, they are obtained from either historical data or building simulation. In Fig. 23, we show a simulation for the hourly internal load at the Pinkafeld test site based on occupancy and equipment.

employees		1	2	3	4	5	6	7	8	9	10	11	12	13	14	15	16	17	18	19	20	21	22	23	24
Monday	kW_{th}	6.0	6.0	6.0	6.0	6.0	6.0	20.4	22.4	24.4	24.4	24.4	22.4	20.4	22.4	24.4	24.4	22.4	18.4	6.0	6.0	6.0	6.0	6.0	6.0
Tuesday	kW_{th}	6.0	6.0	6.0	6.0	6.0	6.0	20.4	22.4	24.4	24.4	24.4	22.4	20.4	22.4	24.4	24.4	22.4	18.4	6.0	6.0	6.0	6.0	6.0	6.0
Wednesday	kW_{th}	6.0	6.0	6.0	6.0	6.0	6.0	20.4	22.4	24.4	24.4	24.4	22.4	20.4	22.4	24.4	24.4	22.4	18.4	6.0	6.0	6.0	6.0	6.0	6.0
Thursday	kW_{th}	6.0	6.0	6.0	6.0	6.0	6.0	20.4	22.4	24.4	24.4	24.4	22.4	20.4	22.4	24.4	24.4	22.4	18.4	6.0	6.0	6.0	6.0	6.0	6.0
Friday	kW_{th}	6.0	6.0	6.0	6.0	6.0	6.0	20.4	22.4	24.4	24.4	24.4	22.4	20.4	20.4	20.4	20.4	19.4	18.4	11.6	11.6	11.6	11.6	6.0	6.0
Saturday	kW_{th}	6.0	6.0	6.0	6.0	6.0	6.0	11.5	11.6	12.0	12.0	12.0	11.6	11.6	11.6	11.6	11.6	11.6	11.6	6.0	6.0	6.0	6.0	6.0	6.0
Sunday	kW_{th}	6.0	6.0	6.0	6.0	6.0	6.0	6.0	6.0	6.0	6.0	6.0	6.0	6.0	6.0	6.0	6.0	6.0	6.0	6.0	6.0	6.0	6.0	6.0	6.0

Figure 23: Pinkafeld Internal Loads

Natural infiltration is accounted for by Eq. 29:

$$\varpi_d^t = \Omega_{\text{vent}}^t \cdot \rho_{\text{air}} \cdot \gamma_{\text{air}} \cdot \left(\Lambda^t - \chi^t\right), \forall\ t \in \mathcal{T}, d \in \mathcal{D}_I \quad (29)$$

The additional nomenclature associated with this equation is as follows:

- Ω^t_{vent}: flow rate for air to HVAC system during period $t \in \mathcal{T}$ (m^3/s)
- ρ_{air}: specific density of air (kg/m^3)
- γ_{air}: specific heat capacity of air (kJ/kg·K)

Finally, we account for heat requirements for air conditioning by relying on the survey of 43 different types of HVAC systems in DIN (2007). First, we determine the enthalpy of the inlet and outlet air as follows:

$$ho^t = 1.01\chi^t + xo^t \cdot \left(2501 + 1.86 \cdot \chi^t\right), \forall\, t \in \mathcal{T} \tag{30}$$

$$hi^t = 1.01\Lambda^t + xi^t \cdot \left(2501 + 1.86 \cdot \Lambda^t\right), \forall\, t \in \mathcal{T} \tag{31}$$

The additional nomenclature associated with these equations is as follows:

- ho^t: enthalpy of humid air outside the building during period $t \in \mathcal{T}$ (kJ/kg)
- hi^t: enthalpy of humid air inside the buildnig during period $t \in \mathcal{T}$ (kJ/kg)
- xo^t: amount of water per unit of external air (kg/kg)
- xi^t: amount of water per unit of internal air (kg/kg)

Consequently, the thermal heat loss through the HVAC system is given by Eq. 32:

$$\varpi^t_d = \Omega^t_{\text{vent}} \cdot \rho_{\text{air}} \cdot \left(\gamma_{\text{air}} \cdot \left(\chi^t - \Lambda^t\right) - EE \cdot \left(hi^t - ho^t\right)\right), \forall\, t \in \mathcal{T}, d \in \mathcal{D}_A \tag{32}$$

The only new term here is EE, which is the efficiency of the heat recovery.

Once it is possible to calculate Ξ^t for each hour under the current building configuration, the heating (if $\Xi^t > 0$) or cooling (if $\Xi^t < 0$) demand for that hour is obtained. Summing each of these up over the entire year, we estimate the annual heating and cooling demands with the current building configuration. Next, in order to estimate the impact of each passive-measure portfolio on end-use energy consumption, we repeat the procedure but with the parameters of the passive measures in each portfolio replacing the ones in Eqs. 26 through 32. Consequently, the annual heating and cooling demand under each passive-measure portfolio may be obtained. Finally, taking the difference and dividing by the original demand yields the percentage reduction in each type of demand. Repeating this exercise for each candidate portfolio, thus, yields the parameters $OD_{k,j}$.

Appendix C: Treatment of Part-Load Efficiency for On-Site Generation

The energy-conversion efficiencies of all equipment vary depending on the level of output. In particular, efficiency may be lower if part-load operations are in effect. Although part-load efficiency is reflected in most optimisation models for central-station generation (Conejo et al., 2010), it has not been included in corresponding research at the building level, e.g., addressing generators with capacities of under 100 kW_e. Indeed, our own energy-balance relations assume such constant efficiencies both at the upper and lower levels, e.g., see Eqs.

4 and 21, respectively. Here, we explore the empirical evidence on part-load efficiency for DER.

In Fig. 24, the electrical and thermal efficiencies of a 1 kW_e fuel cell CHP unit appropriate for installation in a single-family dwelling are indicated (Kaarsberg et al., 2000). Although there is some variation in the efficiencies, they are relatively constant as long as the load is more than 20% of the rated capacity, i.e., the electrical efficiency varies between 30% and 35% in this range. Using data from Matic (2007), we obtain a similar conversion efficiency for a gas-fired 14.3 kW_e CHP unit (similar to the one installed at FASAD) in Fig. 25. As for the fuel cell, the electrical efficiency is relatively stable for loads greater than 25% of rated capacity, i.e., they vary between 28% and 35%. On the other hand, some studies have found a more profound effect due to part-load efficiency for small-scale generators. For example, Rahman and Pipattanasomporn (2010) report an efficiency range from 19% to 28% for a 30 kW_e MT between 20% and 100% load (Fig. 26). Furthermore, Bonilla et al. (2008) find similar inefficiencies in gas turbines and some internal combustion engines, although CHP systems are less prone to exhibiting as drastic efficiency losses for low part loads. Overall, there is no clear picture on the effect of part-load efficiencies for small-scale technologies, which is why we feel that our assumption of constant efficiencies in Section 2 is defensible. Nevertheless, we propose an alternative formulation that may take into part-load effiencies by approximating the non-linear curve in Fig. 26 with a piecewise-linear function. Consequently, a stylised adjustment to Eq. 4 may be formulated by first defining additional terminology as follows:

- $ii \in \mathcal{II}_i$: index for part-load input ranges
- $\mathcal{II}_i$: set of part-load input ranges for energy-creating technology $i \in \mathcal{I}$
- $E_{i,ii,k,kk}$: units of energy type $k \in \mathcal{K}_{I,i}$ needed to produce one unit of energy type $kk \in \mathcal{K}_{O,i}$ in energy-creating technology $i \in \mathcal{I}$ over range $ii \in \mathcal{II}_i$ (kWh/kWh_e or kWh/kWh)
- $bb_{i,ii,k}$: lower input level for energy type $k \in \mathcal{K}_{I,i}$ over part-load range $ii \in \mathcal{II}_i$ for energy-creating technology $i \in \mathcal{I}$ (kWh_e or kWh)
- $y^{p,m,t}_{i,ii,k}$: units of energy type $k \in \mathcal{K}$ used in energy-creating technology $i \in \mathcal{I}$ over range $ii \in \mathcal{II}_i$ during period $p \in \mathcal{P}$, $m \in \mathcal{M}$, $t \in \mathcal{T}$ (kWh_e or kWh)
- $z^{p,m,t}_{i,ii,kk}$: units of energy type $kk \in \mathcal{K}$ produced by energy-creating technology $i \in \mathcal{I}$ over range $ii \in \mathcal{II}_i$ during period $p \in \mathcal{P}$, $m \in \mathcal{M}$, $t \in \mathcal{T}$ (kWh_e or kWh)

We remark that $bb_{i,|\mathcal{II}_i|+1,k} = s^p_i \cdot E_{i,|\mathcal{II}_i|,k,kk}$ if $i \in \mathcal{I}_C$ and $bb_{i,|\mathcal{II}_i|+1,k} = G_i \cdot s^p_i \cdot E_{i,|\mathcal{II}_i|,k,kk}$ if $i \in \mathcal{I}_D$. Furthermore, $E_{i,ii,k,kk}$ is non-increasing in ii. Thus, Eq. 4 may be replaced by Eqs. 33 and 34:

$$z^{p,m,t}_{i,ii,kk} = \sum_{k \in \mathcal{K}_{I,i}} \frac{y^{p,m,t}_{i,ii,k}}{E_{i,ii,k,kk}}, \forall\ i \in \mathcal{I}, ii \in \mathcal{II}_i, kk \in \mathcal{K}_{O,i}, p \in \mathcal{P}, m \in \mathcal{M}, t \in \mathcal{T} \tag{33}$$

$$\sum_{k \in \mathcal{K}_{I,i}} \frac{bb_{i,ii,k}}{E_{i,ii,k,kk}} \leq z^{p,m,t}_{i,ii,kk} \leq \sum_{k \in \mathcal{K}_{I,i}} \frac{bb_{i,ii+1,k}}{E_{i,ii,k,kk}},$$
$$\forall\ i \in \mathcal{I}, ii \in \mathcal{II}_i, kk \in \mathcal{K}_{O,i}, p \in \mathcal{P}, m \in \mathcal{M}, t \in \mathcal{T} \tag{34}$$

Finally, we sum up the energy input and output over all the part-load ranges for each energy type in order to determine the total energy input and output:

$$z_{i,kk}^{p,m,t} = \sum_{ii \in \mathcal{II}_i} z_{i,ii,kk}^{p,m,t}, \forall\ i \in \mathcal{I}, kk \in \mathcal{K}_{O,i}, p \in \mathcal{P}, m \in \mathcal{M}, t \in \mathcal{T} \tag{35}$$

$$y_{i,k}^{p,m,t} = \sum_{ii \in \mathcal{II}_i} y_{i,ii,k}^{p,m,t}, \forall\ i \in \mathcal{I}, k \in \mathcal{K}_{I,i}, p \in \mathcal{P}, m \in \mathcal{M}, t \in \mathcal{T} \tag{36}$$

In terms of implementation, we would use auxiliary decision variables that would indicate the operating region and the weighting between consecutive pairs of breakpoints (Winston and Venkataramanan, 2002).

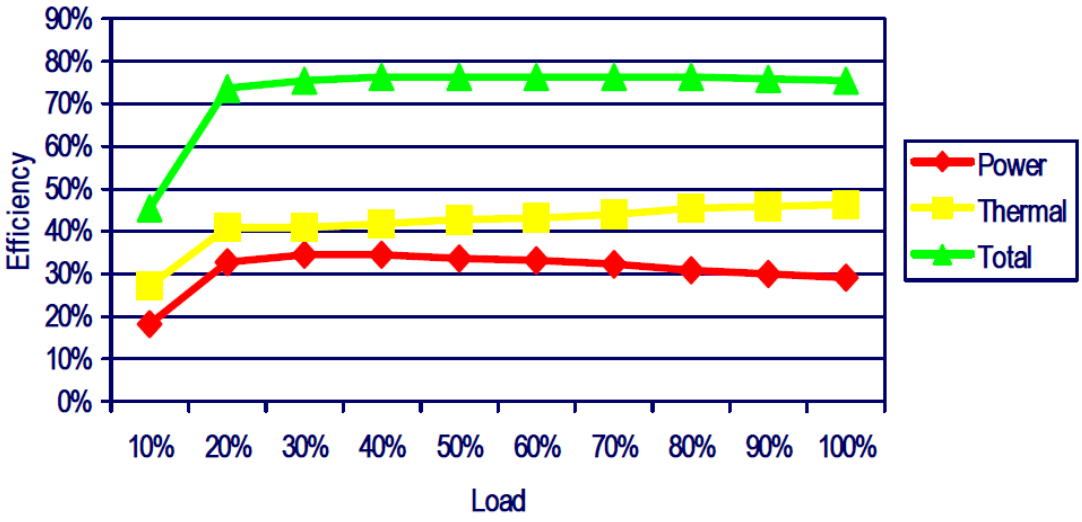

Figure 24: Part-Load Efficiency for a Fuel Cell CHP (Kaarsberg et al., 2000)

Investigating other types of DER, Bonilla et al. (2008) find that the operating temperature may also affect some generators, boilers, heat pumps, and storage equipment more than others. However, since we proposed in the EnRiMa DoW to handle this issue via sensitivity analyses, we feel that incorporating the effect of operating temperatures on the energy output at the upper level of the operational module is beyond the scope of the project.

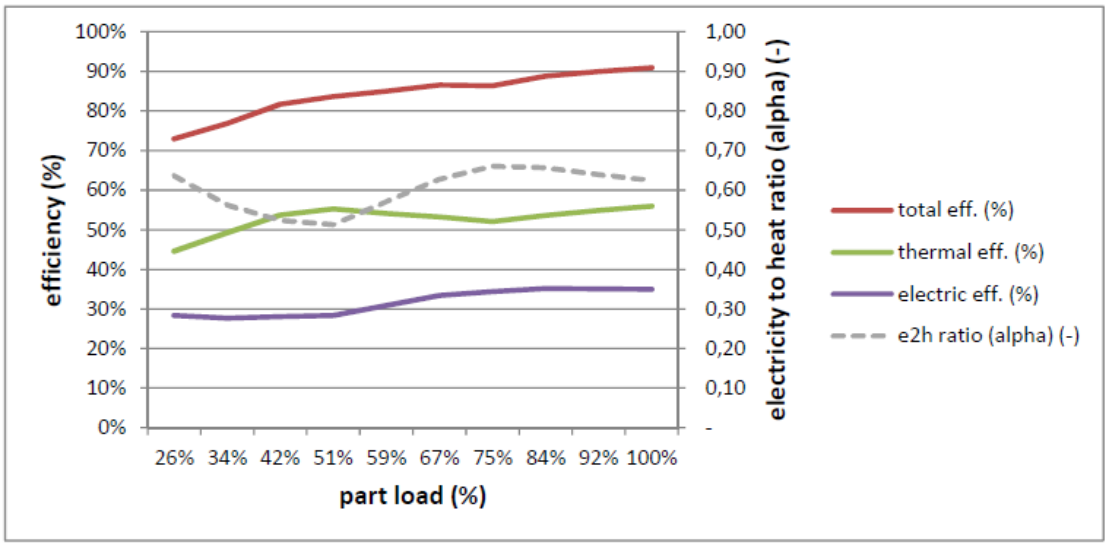

Figure 25: Part-Load Efficiency for a 14.3 kW_e CHP Unit (Matic, 2007)

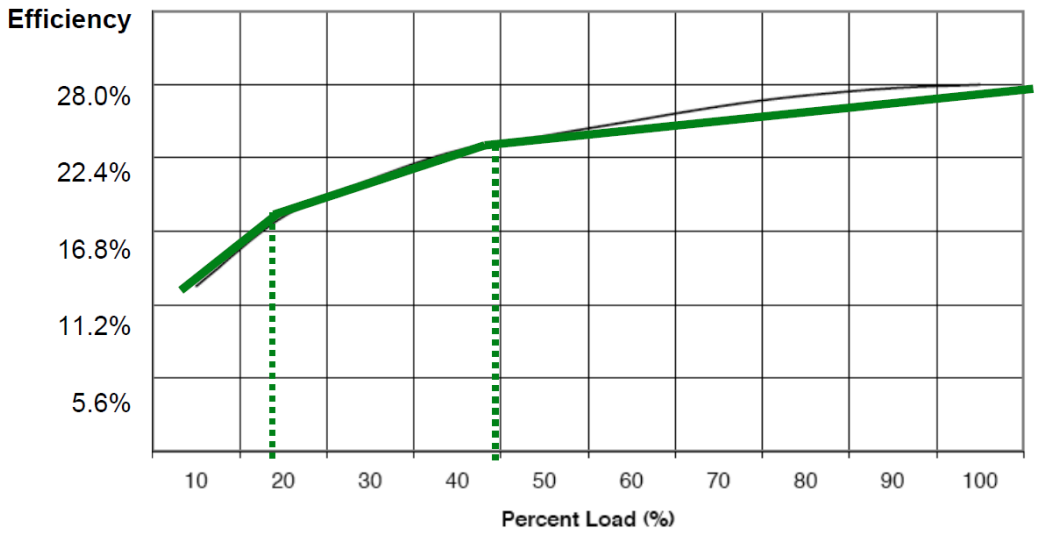

Figure 26: Part-Load Efficiency for a 30 kW_e MT (Rahman and Pipattanasomporn, 2010)